Investigating the Role of *Chlamydia* Putative Cytotoxins During Female Genital Tract Infection

by

Lucie Helene Berclaz

A Paper Presented to the

Faculty of Mount Holyoke College in

Partial Fulfillment of the Requirements for

The Degree of Bachelor of Arts with

Honor

Department of Biological Sciences

South Hadley, MA 01075

May 2025

This paper was prepared

under the direction of

Professor Rebeccah Lijek

for eight credits

ACKNOWLEDGEMENTS

I would like to thank my thesis advisor, PI, and mentor Rebeccah Lijek for the continuous support she has given me throughout this investigation and during my three years working in her lab. My growth as a researcher would not have been possible without her help and I am extremely grateful for all she has taught me. I would also like to thank Kenneth Fields and his lab for their collaboration on this project. Without their contribution of the mutant strain, we would not have been able to perform this research.

I would like to thank the technicians at the Rodent Histopathology Core at Harvard Medical school for processing our samples in record time, and Heather Hamilton for helping us develop our imaging analysis technique. Thank you to the NIH R21 AI78108 grant which gave us the funding for this project and allowed for the research to be possible.

Thank you to the entire Lijek lab for their contributions to this project and the endless support they have given me. I would especially like to express my gratitude to the pathology crew: Akosua Frimpong, Aria Mallare, Grace Wieselquist and Ashna Mehta. Your tireless work at the microscope made all of the difference in this project, you are each incredible and I am so thankful for you as people and as researchers. Thank you to all of the past Lijek lab members whose research laid the groundworks for this project, especially Kyra Seiger, Madison Dresler, Shannon Breen and Da'Vonti Hardrick. Madison and Shan, your support and friendship was one of the primary reasons I fell in love with research,

thank you both for being my rock throughout our time in the lab together. Thank you to Sarah Bacon and Marta Sabariego for serving on my committee and helping me grow as a student and a critical thinker throughout the classes I've taken with them.

Thank you to my friends, who I could not have done this without. Kamlyn, Hannah and Lauren, working on my thesis with you all was one of the highlights of my senior year. To Gracie, who was there with me every step of the way, since our first year, I am forever grateful.

Last but not least, thank you to my parents, my siblings, my dog, and the Mount Holyoke volleyball team (my second family) who have given me the love and encouragement necessary for me to thrive in academics, who have stayed up late with me countless nights to discuss this thesis and my research, who have supported me through every single moment in the lab and in life, and who I wouldn't have been able to do this without. I love you all.

TABLE OF CONTENTS

LIST OF FIGURES

ABSTRACT

Chlamydia is the leading cause of bacterial sexually transmitted infections across the globe. Acquisition of the bacteria often results in asymptomatic chronic infections that can lead to the development of devastating conditions such as pelvic inflammatory disorder and ectopic pregnancy. In spite of the severity and prevalence of *Chlamydia*, how the bacteria causes this disease continues to remain unclear. Previous studies have implicated that a set of open reading frames (ORFs) within the bacteria's genome may contribute to the bacteria's pathogenesis. However, how exactly they contribute has yet to be explored in vivo. In this study, we investigate the role that these ORFs play during *Chlamydia* infection of the upper genital tract. To do so, we infected mice with a mutant strain of *Chlamydia* that lacked these ORFs, and assessed the ability of the bacteria to both infect the host tissue and induce pathology. We found that infection with the mutant strain resulted in reduced oviduct pathology, and reduced persistence of the bacteria in the lower genital tract. These results strongly suggest that these open reading frames act as virulence factors during *Chlamydia* infection that drive oviduct pathology by taking on two different tissue specific mechanisms of action

INTRODUCTION

1. Study Rationale

Chlamydia trachomatis is a Gram-negative bacterium that is the leading cause of bacterial sexually transmitted infections (STI) worldwide (1, 2). While capable of infecting various parts of the body including the eyes and lymph nodes, Chlamydia poses its greatest threat upon infection of the female genital tract (3, 4).

If detected, *C. trachomatis* is readily treatable with antibiotics such as doxycycline or azithromycin, however infection of the genital tract often presents asymptomatically (2). Without treatment, acute *C. trachomatis* infection can develop into chronic infection that persists for years and results in the development of a number of debilitating conditions such as pelvic inflammatory disease, cervicitis, endometriosis and perihepatitis (2,4). These sequelae are frequently accompanied by intense pain in the abdomen and pelvis and also can have devastating consequences for an individual's fertility and reproductive health, as they often lead to ectopic pregnancy and tubal infertility (4).

It has long been understood that the development of these chronic conditions is the result of persistent inflammation and tissue damage caused by the immune response of infected individuals, known as immunopathology (5,6). However, despite the vast number of studies that have been performed with the goal of identifying virulence factors of the bacteria – features that contribute to its

pathogenesis – how exactly *Chlamydia* triggers this immunopathology and causes disease remains unelucidated (2).

There are a variety of subtypes of Chlamydia trachomatis, called serovars, and their ability to cause immunopathology in the female genital tract varies (3). Previous research has identified that types of *Chlamydia* that elicit robust immunopathology of the upper genital tract all share homologous genes that are lacking in the types that do not cause immunopathology (5, 7). These genes, e.g. *CT166* in *C. trachomatis* serovar D and *tc0437-0439* in *C. muridarum*, contain similar genomic sequences to known cytotoxins of other pathogenic bacteria, and have been heavily implicated in the ability of those bacteria to induce immunopathology and cause disease (7). However, despite these strong implications, neither *CT166* nor *tc0437-0439* have been extensively studied, and little to no research has gone into exploring the role of these genes via an animal model.

Thus, the goal of this study is to test whether or not these putative cytotoxin genes serve as virulence factors during *Chlamydia* infection of the female upper genital tract, and to gain insight into how exactly they aid pathogenesis of the bacteria. We will accomplish this by removing these genes from the bacteria's genome and testing the resulting mutant bacteria in a mouse model to assess how their deletion impacts the ability of *Chlamydia* to both infect the genital tract and induce immunopathology (Figure 1).

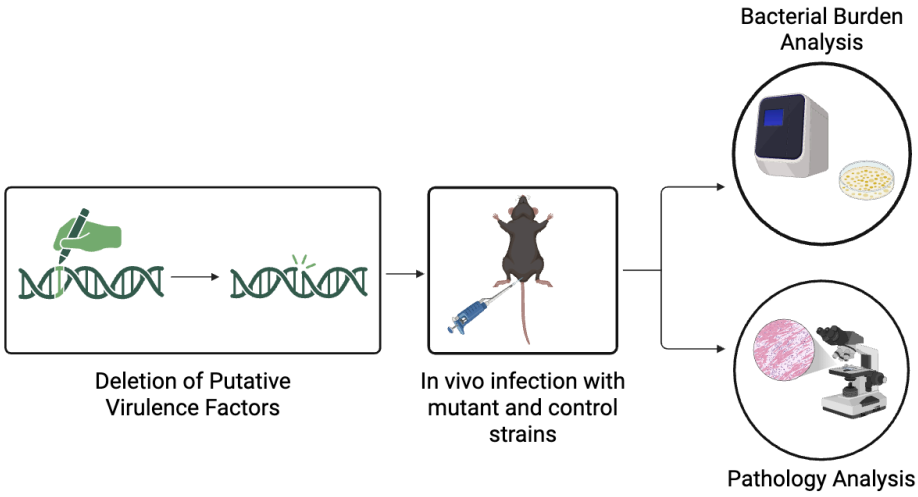

Figure 1. Schematic diagram outlining the rationale of this study. A mutant strain of *Chlamydia* will be generated that lacks the open reading frames encoding the putative virulence factors. Mice infected with the mutant and control strains will then be assessed for bacterial burden and pathology. Figure created with BioRender.

The severe implications of *C. trachomatis* infection on reproductive health coupled to the fact that there are 128.5 million new cases of chlamydial disease annually means that it is of the utmost importance that the pathogenesis of the bacteria be identified (1). Evaluating the role of putative cytotoxin genes during *Chlamydia* infection will help to gain insight into how this disease can be prevented.

2. *Chlamydia* infection of the genital tract

The *Chlamydia* genus consists of a number of distinct species of the bacteria that infect various organisms at different anatomical sites (6). *Chlamydia trachomatis* is one of the sole species that naturally infects humans, and is the most prevalent form of the bacteria worldwide (8). Within the *C. trachomatis* species itself, there are a number of variants, known as serovars, that differ from one another in terms of the molecules they present on their surfaces, called antigens. Infection location and severity are serovar specific, and thus are often highly varied depending on which serovar individuals are infected with. *C. trachomatis* exists as fifteen different serovars (lettered A through K), that fit within three distinct categories, or biovars, based on the location of the body that they invade: serovars A-C infect epithelial cells of the eye, serovars D-K infect epithelial cells of the urogenital tract, and serovars L1-L3 infect the lymph tissue of the genital tract (2, 6). Of these three distinct biovars, invasion of the urogenital tract with serovars D-K is the most common type of chlamydial infection, and has been linked to higher rates of disease severity (2).

Genital tract infection begins with *Chlamydia* infecting the columnar epithelial cells of the cervical lining (9). From there the bacteria can ascend, spreading to the upper genital tract, invading the uterus, fallopian tubes, and ovaries as the infection progresses. The asymptomatic nature of infection with *C. trachomatis* D-K leads to chronic inflammation of the upper genital tract, causing tissue damage that often leads to fibrosis, the accumulation of scarred connective

tissue (10). The presence of fibrosis in the female upper genital tract frequently leads to the build up of fluid within the fallopian tubes, a condition known as hydrosalpinx (Figure 2) which typically leads to acute reproductive damage and ectopic pregnancy (11).

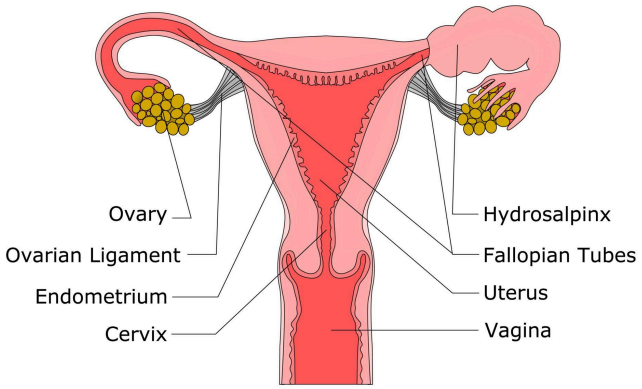

Figure 2. Diagram of hydrosalpinx within the human genital tract. Blockage in the fallopian tube results in fluid accumulation and swelling of the reproductive tissue. Figure adapted from FERTi-JiN.

3. Studying *Chlamydia* Infection

Due to the location and severity of infection, studying *C. trachomatis* and how it causes disease in the upper genital tract in humans is not often feasible, and instead typically relies on the use of animal models. Mouse models are the most commonly used method of studying *Chlamydia* infection due to (a) their practicality (low cost and high availability) (b) their susceptibility to genital tract infection with different chlamydial species (c) their similarities in genital tract

anatomy to humans (Figure 3A), and (d) that the progression of genital tract infection in mice mimics genital tract infection in humans (12, 13). However, a critical limitation of the murine model lies in the fact that vaginal infection with *C. trachomatis* does not consistently ascend to the upper genital tract nor elicit the same robust mucosal immunopathology associated with *C. trachomatis* infection in humans (13). To overcome this limitation, research has often turned towards using other species of the bacteria that closely resemble *C. trachomatis* and are capable of establishing an ascending infection in the murine genital tract.

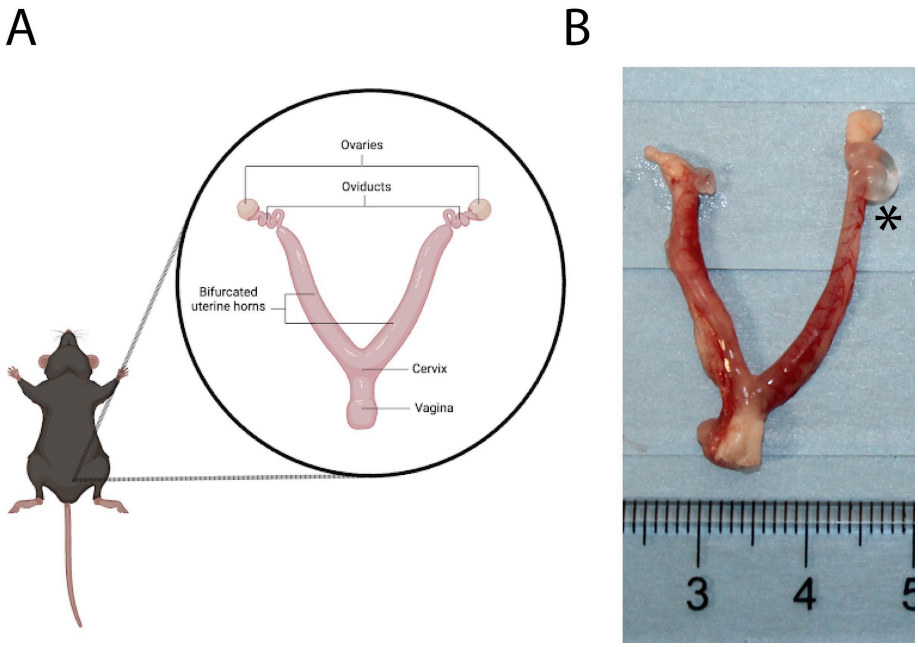

Figure 3. Murine Genital Tract Overview (A) Anatomy of the murine genital tract. The lower genital tract of the tissue is composed of the vagina and cervix. The upper genital tract consists of two uterine horns, each of which are connected to an ovary via a tube known as the oviduct, which serves a function homologous to that of the fallopian tubes in humans. (B) Excised mouse uterus 51 days post transcervical infection with *C. muridarum*. Hydrosalpinx, marked by a black

asterisk, is present in the right oviduct, evident by its clear, glasslike appearance. Image was taken by Hattie Nichols in the Lijek Lab.

Chlamydia muridarum is a mouse species of *Chlamydia* that shares genomic sequence similarity with the human pathogen *C. trachomatis*. Similar to *C. trachomatis* serovars D-K, *C. muridarum* readily infects the genitourinary tract and leads to the establishment of acute immunopathology (12). Murine infection with *C. muridarum* very closely mimics *C. trachomatis* infection in humans, with the bacteria initially invading the lower murine genital tract before ascending to the upper genital tract tissue, where it prompts the development of uterine dilation and extreme hydrosalpinx characterized by "glass ovaries", seen in Figure 3B (13). The *C. muridarum* model of infection in mice has played a critical role in understanding both *Chlamydia* pathogenesis and the host immune response to *Chlamydia* genital tract infection, and thus serves as a practical and valuable method of indirectly studying the human pathogen and how it causes disease. In this study, we use *C. muridarum* infection of the mouse to model human *C. trachomatis* disease.

4. Overview of the Immune System

After both human and mouse *Chlamydia* infection, the disease is driven by the immune response to infection. The immune system is a diverse yet highly efficient network of cells, tissues and molecules that work together to protect the body against foreign invaders (14). Despite its complexity, the immune system

can be divided into two central components: the innate system and the adaptive system.

4.1 Innate immunity

A non-specific rapid response to a pathogen, the innate immune system is a combination of anatomical barriers and cellular responses, and serves as the body's first line of defense against invaders. When a pathogen first enters the body, it encounters a number of physical barriers, such as mucous membranes or epithelial layers of the skin. To establish an infection it must not only traverse through these obstacles, but also survive the acidic pH and antimicrobial peptides present at these barriers. If it is capable of overcoming these and establishing an infection, the next phase of the innate immune response, the cellular response, is triggered (14).

When white blood cells patrolling throughout the body encounter the pathogen, they recognize the presence of foreign molecules known as antigens on the pathogen surface. Upon this recognition, they recruit other white blood cells such as neutrophils, macrophages, natural killer cells and dendritic cells to the site of infection via the release of chemical messenger molecules known as cytokines. These various innate cells either engulf and destroy the invader in a process known as phagocytosis, opsonize and mark it for future destruction, or take up antigens in preparation for activation of the adaptive immune response (15). The goal of the innate immune system is to quickly detect and respond to a pathogen

so that the body can either clear the invader immediately, or mount a larger scale immune response if necessary. The innate system is nonspecific, it cannot generate a targeted attack against a particular pathogen, and thus often is not enough to clear an infection on its own.

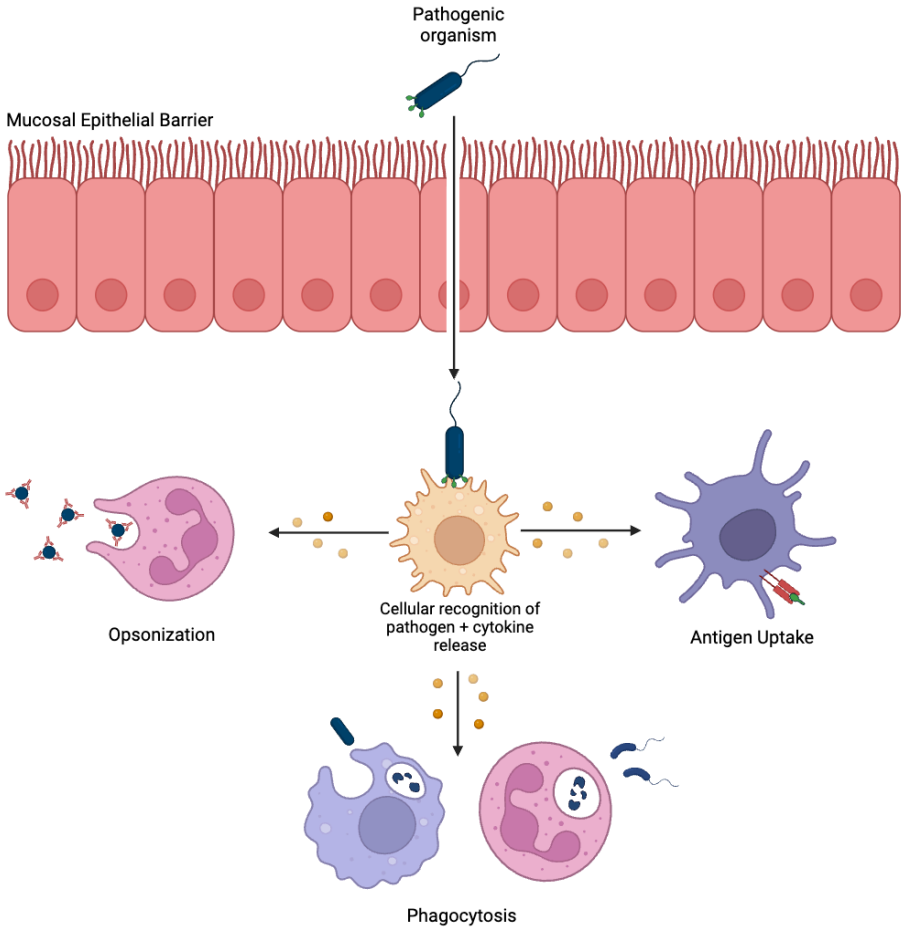

Figure 4. Pathways involved in the innate immune response to infection. Pathogens first encounter physical and chemical barriers before being recognized and attacked by white blood cells such as neutrophils, macrophages and dendritic cells. Figure created with BioRender.

4.2 Adaptive Immunity

The adaptive immune system is the second line of defense against a pathogen that has already established an infection. A targeted response to a specific pathogen, the adaptive system is composed primarily of two cell types: B lymphocytes and T lymphocytes, which are activated via the presentation of antigens to them by cells of the innate system such as dendritic cells or macrophages (15). Once activated, B lymphocytes either differentiate into plasma cells, or memory cells. The role of plasma cells is to produce antibodies, small molecules that attach to pathogens and either neutralize them or mark them to be phagocytosed in a process known as opsonization. Memory B cells do not actively contribute to the clearance of a pathogen, but are critical in establishing immunological memory. Once an infection has been cleared, most immune cells will die, but antigen specific memory B cells survive and take up residence in lymph tissues where, upon a secondary infection with the same pathogen, they can proliferate and easily mount a targeted efficient attack before the microbe can properly establish an infection (14). Similar to B lymphocytes, T lymphocytes differentiate into different cell types once activated, either serving as T helper cells (CD4+) or cytotoxic T cells (CD8+). T helper cells coordinate inflammation, regulate immune cell development and help the recruitment of immune cells to the infection site. Cytotoxic T cells recognize host cells that have been infected with a pathogen, and eliminate them by releasing cytotoxic granules and inducing apoptosis (15).

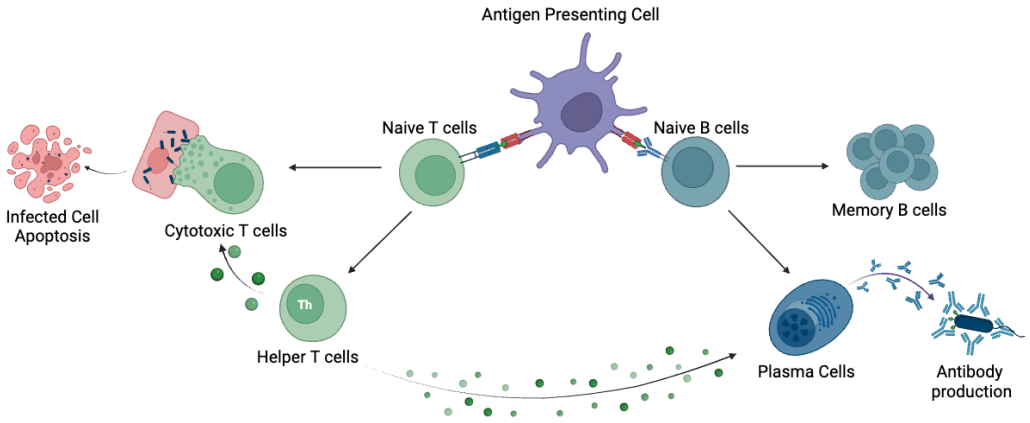

Figure 5. Diagram of the adaptive immune response to infection. The adaptive immune response mounts a targeted response against the pathogen through the activation of B and T lymphocytes upon antigen presentation. Figure created with BioRender.

Clearance of a pathogen requires the innate and adaptive systems to work cohesively with one another in order to mount a robust immune response to fight infection. However, this immune response is not always beneficial for the infected host, and instead can be incredibly debilitating if it leads to the development of immunopathology. Characterized by persistent inflammation and tissue damage, immunopathology is caused by excessive immune cell recruitment to the infected tissue. The line between a productive and a harmful immune response depends on the infected individual and the pathogen responsible for the infection, and at times both types of responses are generated (14, 6).

5. Host response to *Chlamydia* infection

Previous research in the Lijek lab has identified that serovars of *C. trachomatis* which infect the female upper genital tract induce two independent immune responses (5). One of the immune responses is protective, and is actively involved in clearance of the bacteria. The other is non protective and does not aid in the elimination of the bacteria, but instead attacks the tissue of the upper genital tract, resulting in the development of immunopathology and the disease state associated with *Chlamydia* infection (5, 16). Once *Chlamydia* has entered host cells and begun to spread throughout the female genital tract, both types of immune responses are initiated, each of which are characterized by an influx of distinct immune cells to the site of infection.

5.1 Protective Response

The protective immune response relies on a number of different cell types including B cells and CD8+ cells, but is primarily led by a subset of CD4+ cells known as T Helper 1 (Th1) cells (16). Via the promotion of macrophage activation, naive T cell differentiation, and the production of pro-inflammatory cytokines such as interferon gamma (IFN-γ), Th1 cells actively eliminate the infection, depriving it of nutrients, coordinating the lysis of infected cells, and flushing out the bacteria (17).

5.2 Non protective Response

The non protective immune response during chlamydial infection is characterized by the recruitment of neutrophils and non-specific CD4+ cells and CD8+ cells to the site of infection (5). These cells – instead of coordinating with the protective immune response to fight off the bacteria – do not contribute to infection clearance, and instead drive immunopathology and disease within the host.

Neutrophils are one of the first cells recruited to the reproductive tract upon *Chlamydia* infection, invading the lumenal space of the uterus and contributing to prolonged tissue damage once they arrive (Figure 6A, 6C). Dysregulation and excessive activation of neutrophils in response to the bacteria results in the secretion of a variety of molecules that degrade and damage surrounding cells and tissue: (a) reactive oxygen species which promote inflammation and impair host cells, and (b) matrix metalloproteinases that degrade the extracellular matrix surrounding cells and contribute to fibrosis and scarring (5, 18). CD4+ and CD8+ cells are recruited to the genital tract tissue in the later stages of infection, however their role in inducing immunopathology is not as well understood. Studies using mouse models suggest that CD4+ and CD8+ cells that are not specific for Chlamydia antigens (“bystander” T cells) can infiltrate the epithelial layers of the genital tract tissue (Figure 6B). Bystander T cells lack antigen specificity, and thus lack the ability to recognize and clear the bacteria. These nonspecific lymphocytes have been implicated in other chronic

inflammatory diseases as cells that induce pathology, however the mechanisms that they utilize to do so during chlamydial infection remain unclear (5, 19).

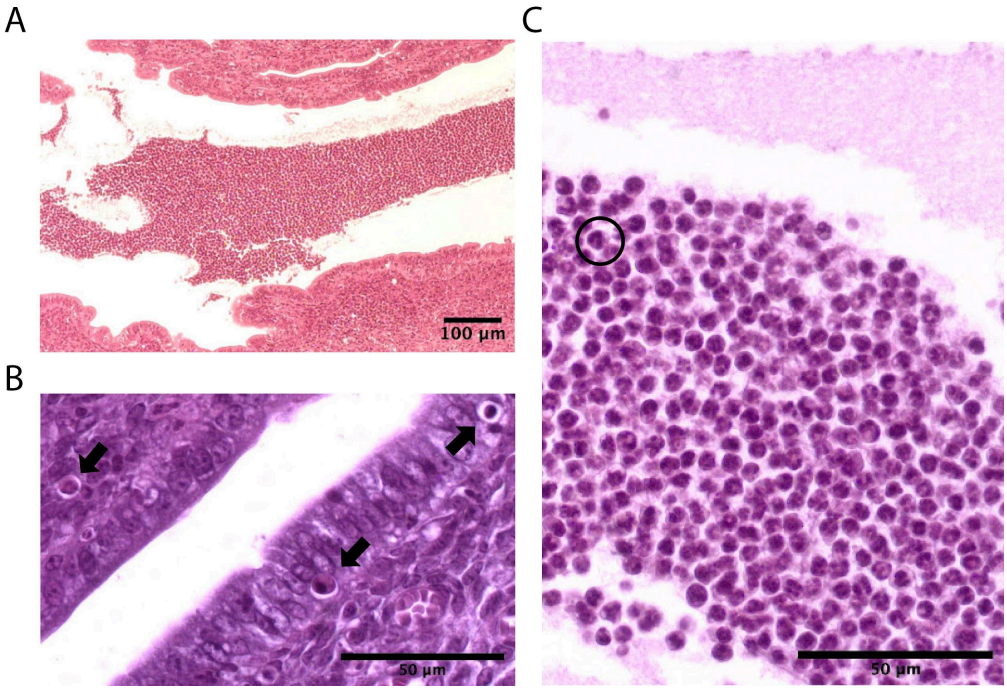

Figure 6. Immune cells of the non protective immune response. (A) Immune cell infiltration of the murine uterine horn post infection with *C. trachomatis*. (B) Presence of lymphocyte cells within the epithelium of the murine uterine horn post infection with *C. trachomatis*. Lymphocytes are marked with black arrows. (C) Neutrophil invasion of the uterine horn. Neutrophils are evident by their multilobed nuclei, with a clear nuclei circled in black. Images were acquired on a Nikon Eclipse 50i microscope at Mount Holyoke College at 10x (A) or 40x (B,C) magnification.

The non protective immune response persists within the infected host even after the initial infection of the bacteria has been cleared. Chronic invasion of the upper genital tract by these three cell types leads to an accumulation of cell and tissue damage which triggers further immune cell recruitment to the infection site,

creating a positive feedback loop of inflammation that perpetuates and exacerbates immunopathology (5). As a result, cellular infiltration of the upper genital tract causes a number of morphological changes in the tissue: thickening and separation of the ovarian membrane (Figure 7A); infiltration of mucus into the lumenal space of the uterine horns and oviducts (Figure 7B) ; fluid build up that results in uterine dilation and oviduct edema (Figure 7C); and hydrosalpinx (Figure 7D).

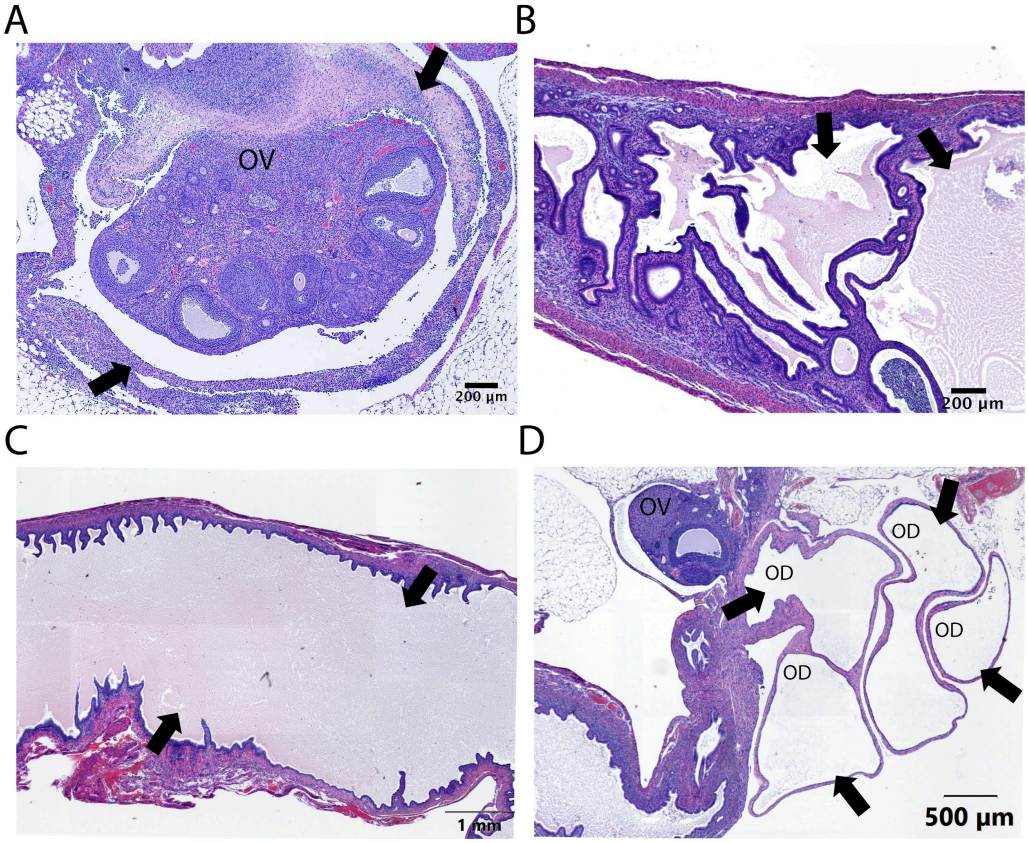

Figure 7. H&E stained mouse genital tract tissue after infection with *C. muridarum*. (A) Thickening of and separation of the ovarian membrane. Ovarian membrane marked by black arrow, ovary marked by OV. (B) Mucus infiltration into the lumenal space of the uterine horns. Lumenal space marked by black arrow. (C) Dilation of the uterine horn. Lumenal space marked by black arrow.

(D) Hydrosalpinx, the extreme swelling and build up of fluid within the tissue of the oviduct. Hydrosalpinx marked by black arrows, oviducts marked by OD.

6. Cellular mechanism of infection

The ability of *Chlamydia* to elicit a robust non protective immune response is contingent upon the ability of the bacteria to infect host cells. All species of *Chlamydia* are obligate intracellular pathogens that survive within humans by entering and invading host cells. Once inside, the bacteria exploits cell nutrients and machinery in order to replicate, spread, and cause disease (2). This manner of infection is highly efficient yet incredibly complex, and relies on the presence of various features of the bacteria, one of which is its unique life cycle. *Chlamydia* has a biphasic developmental cycle which consists of the bacteria shifting between two different forms: The metabolically inactive yet infectious Elementary Body (EB) form, and the non-infectious yet replicative Reticulate Body (RB) form (2, 20).

The bacteria enters host epithelial cells while in its infectious EB form, via the binding of EB membrane proteins to host cell receptors. These binding interactions tether the bacteria to the host and in doing so facilitate the penetration of needle-like projections of the bacteria - known as the Type 3 Secretion System (T3SS) - into the host cell membrane (20). Once the membrane has been punctured, the T3SS secretes effector proteins that accomplish a number of tasks, one of which is to reorganize the actin cytoskeleton of the host cell. This actin remodeling allows for the bacteria to be internalized and endocytosed into the

host cell, in which it remains enclosed within a membrane bound vacuole known as the inclusion (2, 20).

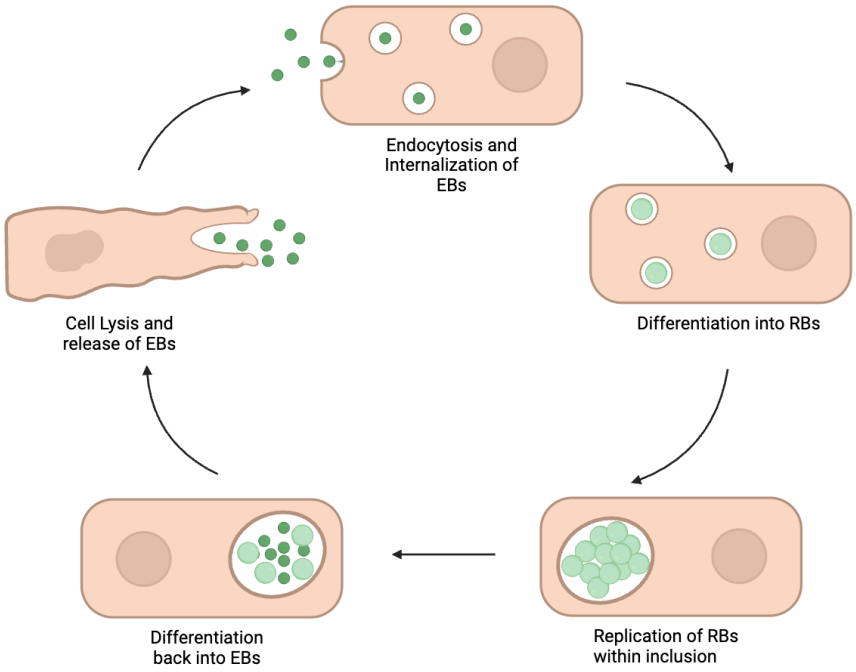

Figure 8. Schematic representation of chlamydial infectious cycle. Figure created with BioRender.

Within the inclusion, the bacteria differentiates from the EB to the RB form. RBs, while incapable of infecting and entering cells, are metabolically active and so are able to replicate rapidly. With the aid of the secreted T3SS effector proteins, which sequester nutrients from the host and take control of biological pathways to ensure the cell enters an anti-apoptotic state, *Chlamydia* RBs divide rapidly via binary fission (2, 4). Repeated replication changes the

environment of the cell**;** ATP availability decreases, cellular nutrients begin to deplete, and the available volume within the inclusion diminishes. Under these conditions, RBs differentiate back into EBs, and exit the host either through exocytosis of the inclusion or through cell lysis (4). Once in the extracellular space, the newly formed EBs come into contact with neighboring cells, presenting them with the opportunity to repeat their infectious cycle, and spread throughout the host (2).

7. A putative *Chlamydia* cytotoxin

The ability of *Chlamydia* to cause disease arises due to the many virulence factors of the bacteria that facilitate its ability to infect and attack host cells. However, the molecular pathogenesis of *Chlamydia* that induces the non protective immune response of the host and drives immunopathology has yet to be fully understood. It has long been hypothesized that *Chlamydia* Elementary Bodies (EBs) express a large putative cytotoxin – a protein that damages and kills host cells by altering the cell cytoskeleton – that serves as a critical virulence factor of the bacteria during genital tract infection (21).

Despite the many species and serovars that exist within the *Chlamydial* genus, only three forms of the bacteria readily infect the genital tract: *C. trachomatis* serovars D-K, *C. trachomatis* serovars L1-L3, and *C. muridarum* (2,3). Upon infection, both *C. muridarum* and serovars D-K establish an acute infection and elicit robust immunopathology characterized by an influx of

neutrophils and intraepithelial lymphocytes to the upper genital tract. In comparison, infection with L1-L3 evokes a milder and fleeting inflammatory response in which immune cell infiltration of the reproductive tract tissue is markedly reduced (5). The genomes of serovars D and L2 – the *C. trachomatis* serovars with the highest incidence of human infection within their biovars – as well as *C. muridarum,* are highly conserved with one another, both in regards to gene content and gene order (5, 7) However, there is one region of the genome, known as the plasticity zone, that is remarkably variable across the three strains (22).

Of the three strains of the bacteria, the plasticity zones of serovar D and *C. muridarum* most closely resemble one another, varying slightly in size and in how many open reading frames (ORFs, which are regions of DNA that encode for proteins) they contain, however still remaining remarkably similar to one another (Figure 9). The plasticity zone of *C. trachomatis* serovar D contains an open reading frame known as *CT166*, which is homologous to three ORFs found in the *C. muridarum* plasticity zone: *tc0437*, *tc0438*, and *tc0439*. These ORFs, the three in *C. muridarum* and the one in *C. trachomatis* D, notably share sequential homology with known cytotoxins TcdA and TcdB of the pathogenic bacteria *Clostridium difficile* (7).

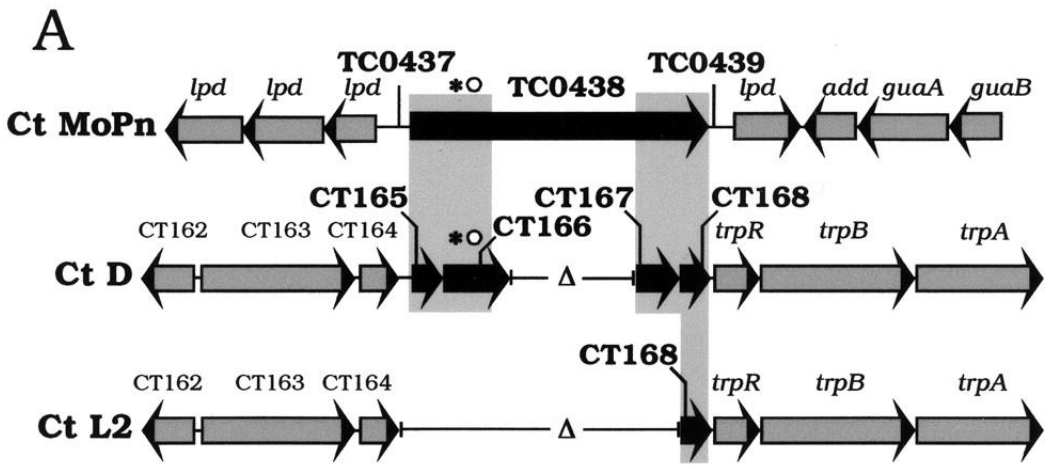

Figure 9. Open reading frames present within the plasticity zones of the three strains of genital *Chlamydia* infection, *C. muridarum* (CT MoPn), *C. trachomatis* serovar D (Ct D), and *C. trachomatis* serovar L2 (Ct L2). Homologous regions of the open reading frames are highlighted. Figure was adapted from Belland et al., 2001.

A gram positive bacteria that attacks the gastrointestinal (GI) tract, *C. difficile* colonization triggers inflammation of the gut that is marked by neutrophil recruitment to the GI tissue (23). The secreted cytotoxins TcdA and TcdB are largely considered to be the primary virulence factors of the bacteria, driving the host innate immune and inflammatory response to infection (24). The cytotoxins contain glucosyltransferase activity, and thus are capable of modifying intracellular regulatory proteins via the transfer of glucose molecules. Through these modifications, TcdA and TcdB interfere with downstream biochemical pathways within the cell, disrupting the organization of the actin cytoskeleton,

causing structural damage that induces cell death, and therefore having a cytopathic impact on the host cells they encounter (7, 24).

The glucosyltransferase activity of the *C. difficile* cytotoxins and that of other large cytotoxins is marked by a series of amino acids known as the DXD motif (Figure 10). This motif is highly conserved in the proteins that are encoded for by *CT166* and *tc0437–0439*, suggesting the potential for these proteins to similarly function as glucosyltransferases (25). In comparison to serovar D and *C. muridarum*, serovar L2's plasticity zone notably lacks a homologous open reading frame to *CT166* and *tc0437-tc0439*, and instead contains a large deletion region (Figure 6). This means that the L2 serovar does not share sequential homology to known cytotoxins and does not contain the DXD motif that appears to be critical for glucosyltransferase activity (7).

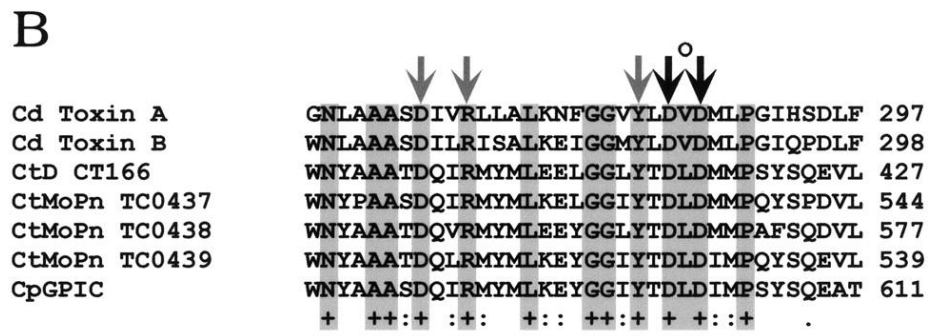

Figure 10. Comparison of amino acid sequence between *C. difficile* cytotoxins (Cd Toxin A, Cd Toxin B) and *Chlamydia* open reading frames *CT166* and *tc0437*, *tc0438* and *tc0439*. Gray arrows indicate amino acid residues that are involved in glucosyltransferase activity, and black arrows indicate amino acid residues required for glucosyltransferase activity. The circle indicates the conserved DXD motif. Highlighted areas mark conserved regions across the different proteins. Figure was adapted from Belland et al., 2001.

The genomic composition of the plasticity zones of the three strains suggests that serovar D and *C. muridarum* have the capacity for cytotoxic behavior upon infection, while L2 likely does not share this capacity. This conjecture has been strongly supported by cell culture studies conducted by Belland et al., reproduced in Figure 11, which observed how infection of HeLa cells with EBs of the three different strains of *Chlamydia* (D, L2, *C. muridarum*) impacted cell morphology. Belland et al identified that cells infected with serovar L2 appeared to have the same morphology as uninfected cells, retaining a normal distribution of actin filaments within their cytoskeleton. In comparison, cells treated with either serovar D or *C. muridarum* displayed an entirely different phenotype, taking on a ballooned appearance marked by cell rounding and the extensive breakdown of the actin cytoskeleton, both of which are attributes closely associated with cytopathic behavior (7). These cell culture studies strongly suggest that EBs of serovars D and *C. muridarum* contain cytotoxic characteristics, and that EBs of serovar L2 do not.

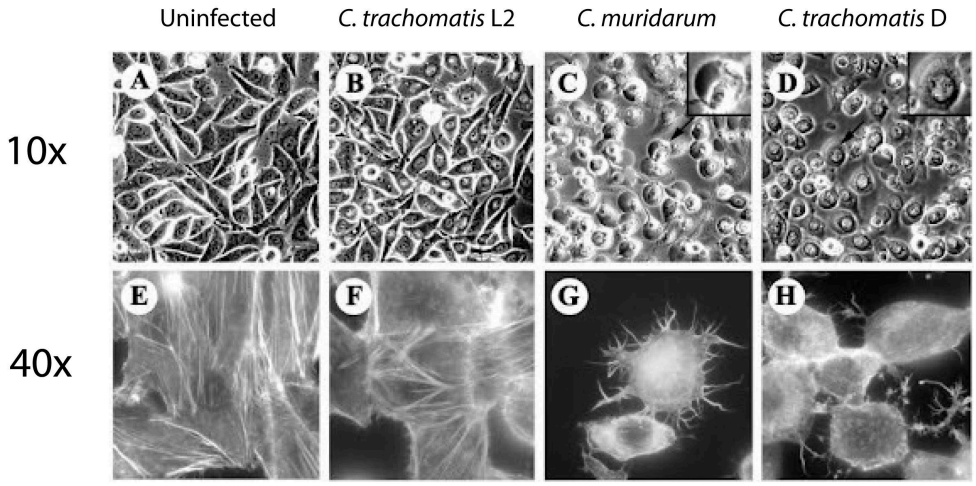

Figure 11. Assessment of cell rounding and actin rearrangement. HeLa cell monolayers were photographed 4 hrs post infection with various strains of *Chlamydia* at 10x or 40x magnification. Cells were either uninfected, infected with *C. trachomatis* L2, infected with *C. muridarum*, or infected with *C. trachomatis* D. Figure was adapted from Belland et al., 2001.

The clear absence of cytotoxicity in serovar L2 indicates that these potential glucosyltransferases, CT166 and tc0437-0439, which are situated in the plasticity zone, the one region of the genome that differs across the three strains, could be the source of their respective strains' virulence. The presence of putative cytotoxin genes in the serovar D and *C. muridarum*, the strains of the bacteria that elicit robust immunopathology, and the absence of these same genes in serovar L2, which only prompts mild immunopathology, strongly suggests that CT166 and tc0437-0439 act as virulence factors that play a role in the ability of their respective chlamydial strain to induce immunopathology.

8. How do CT166 and tc0437-0439 contribute to pathogenesis?

8.1 Role in Host Cell Entry

In order to both infect host cells and maintain the stability of the inclusion, *Chlamydia* must modify and rearrange the host cell actin cytoskeleton (26). Bacterial entry is facilitated by actin polymerization that allows for endocytosis of the bacteria into the cell. However following endocytosis, the bacteria must promote actin depolymerization that returns the actin cytoskeleton to its previous state in order to maintain the morphology of the host cell and retain a space for the bacteria to grow and replicate within. Cell culture studies have shown that CT166 is capable of inducing actin depolymerization and reorganization via the glycosylation of GTPase proteins (27). Thus, it has been proposed that CT166 is a secreted protein that ensures the entry and intracellular survival of *C. trachomatis* within host cells via remodeling of the actin cytoskeleton. Studies performed by the Fields lab at the University of Kentucky, with whom we are collaborating with on this study, have demonstrated that the removal of tc0437-0439 from *C. muridarum* results in decreased invasion efficiency of the bacteria in cell culture. Taken together, these findings suggest that CT166 and tc0437-0439 may play a critical role in the ability of their strains of *Chlamydia* to manipulate the actin cytoskeleton of host cells and initiate infection.

8.2 Role in Immunopathology

Strong evidence also points to the possibility of CT166 and tc0437-0439 playing a role in inducing immunopathology of the upper genital tract. Prior to the commencement of this study, the Lijek lab performed a vaccine trial in which a virus-like particle known as Qβ was chemically conjugated to CT166 peptides, and administered to mice before challenge with *C. trachomatis*. When histopathology of the upper genital tract was assessed post challenge, it was identified that mice given the CT166 vaccine had ameliorated immunopathology in comparison to mice given a Qβ control, marked by a reduced influx of neutrophils and intraepithelial lymphocytes into the upper genital tract (Figure 12). The results of this vaccine study suggest that CT166 and perhaps tc0437-tc0439 may play a role in driving the development of mucosal immunopathology during chlamydial infection.

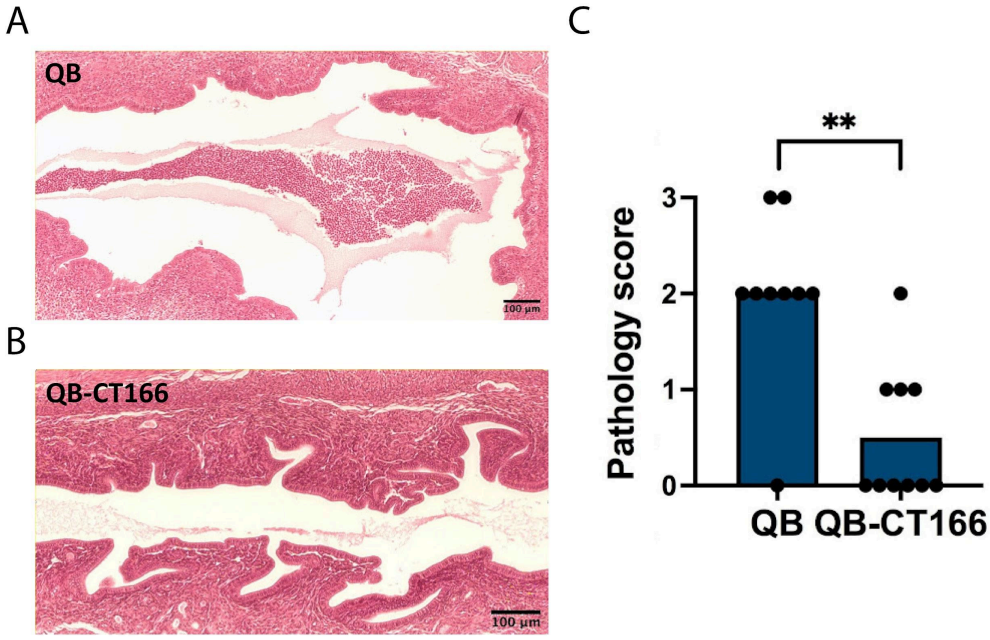

Figure 12. Results of pilot vaccine study. H&E stained mouse uteri challenged with *C. trachomatis* post immunization with (A) a Qβ control vector or (B) a CT166-Qβ vaccine vector. Uterine pathology scores for both groups were assessed externally under anonymized conditions with higher scores being representative of increased immune cell infiltration of the uterine horns and ovaries.

Despite the strong implications of these preliminary studies, the role that *CT166* and *tc0437-0439* play in *Chlamydia* pathogenesis has yet to be identified, and has not been explored in vivo using animal models. Extensive research into these subjects is critical in order to understand how the bacteria causes disease and therefore how this disease can be prevented. Thus addressing these knowledge gaps is the central focus of this study.

9. Research Question and Hypotheses

The aim of this research is to identify how open reading frames *tc0437*, *tc0438* and *tc0439* impact the ability of *Chlamydia muridarum* to cause disease in the female upper genital tract of mice. We hypothesize that these open reading frames serve as virulence factors of the bacteria that drive immunopathology of the upper genital tract and facilitate bacterial entry into host cells.

9.1 Using a Mouse Model

This research will be conducted via the use of a mouse model. Studying *Chlamydia* infection in human tissue is challenging due to the location and severity of infection. To bypass this obstacle, the *Chlamydia* field commonly utilizes a mouse model of infection that acts as a practical alternative to studying human tissue due to ease of handling mice and the similarities between the murine and human female genital tracts (12). Using a mouse model allows for more extensive data collection and reduces variability across subjects by granting control over age, genetics, lifestyle and history, a level of regulation which is difficult to obtain when studying the human population.

9.2 Using *C. muridarum*

Considering the applications of this research in understanding more about human pathogens, it would be most ideal to study CT166, the open reading frame located within the genome of *C. trachomatis* serovar D, the form of the bacteria

that naturally infects humans. However, this is impractical for two reasons: (1) *C. trachomatis* is not readily genetically manipulated, and thus creating a mutant strain of the bacteria in which CT166 has been deleted from the genome has proven unsuccessful during mutagenesis studies thus far, and (2) Infection of the murine upper genital tract with *C. trachomatis* does not elicit the same robust immunopathology that is evident upon infection of the human upper genital tract with *C. trachomatis*. In comparison, *C. muridarum* infection in mice closely resembles *C. trachomatis* infection in humans, making it an effective model to study *Chlamydia* disease (13). Therefore, this research will instead focus on the *CT166* homologous open reading frames *tc0437*, *tc0438* and *tc0439*, using *C. muridarum* and a mouse model of infection to take the first step towards understanding more about these putative virulence factors.

9.3 Assessing Bacterial Burden and Immunopathology

To answer the central questions being posed by this study, we will utilize a mutant strain of *Chlamydia muridarum*, known as *C.muridarum* Δtox , in which the three open reading frames *tc0437*, *tc0438* and *tc0439* have been deleted from the bacteria's genome. Studying strains of the bacteria which are lacking these potentially virulent ORFs allows us to determine how the characteristics of the bacteria and its ability to infect are modulated in their absence. Our research focuses on assessing two critical characteristics of *Chlamydia* infection – the ability of the bacteria to infect, and the ability of the bacteria to elicit

immunopathology – through the quantification of bacterial burden and immunopathology.

Bacterial burden assesses how much of the bacteria is present in the infected tissues, thus indicating the ability of the bacteria to invade host cells and establish infection. We hypothesize that a *C. muridarum* mutant lacking *tc0437-0439* will have reduced bacterial burden in the upper and lower genital tract in comparison to the WT and complemented (cistox) strains of *C. muridarum*. Immunopathology evaluates the degree to which non protective immune cells have infiltrated the infected tissue, thus assessing the robustness of the non protective immune response triggered by the bacteria. We hypothesize that removal of *tc0437-0439* from *C. muridarum* will reduce immunopathology of the upper genital tract in comparison to WT and cistox *C. muridarum*. By using a mouse model to compare how these characteristics of infection change in the absence of *tc0437-tc0439*, this study aims to gain insight into the mechanisms with which these open reading frames contribute to *Chlamydia* infection.

METHODOLOGY

1. Experimental Outline

This study was conducted in two sequential phases. The first of which was a series of preliminary experiments which assessed whether or not a genetic approach was an effective method to dissect the contributions of *tc0437-0439* to *Chlamydia* pathogenesis in vivo. The second was a more comprehensive set of experiments that built off of the results of the first stage and assessed these contributions more extensively. Both phases involved the infection of C57Bl/6 mice with different strains of *Chlamydia muridarum* with the goal of assessing immunopathology and/or bacterial burden. C57Bl/6 mice were chosen as the strain of mouse to be used throughout the study due to their immunocompetency, their inbred nature which ensures identical genotypes, and the frequency with which they are used in the *Chlamydia* field. Two different routes of infection, intravaginal or transcervical inoculation of mice, were utilized in both the preliminary and secondary phases. Intravaginal infections were performed to: (1) mimic the human route of genital tract infection, (2) remain consistent with the route of inoculation typically utilized in the mouse model of *C. muridarum* infection, and (3) investigate specific characteristics of infection such as bacterial ascension, in which the inoculate must be deposited in the lower genital tract. Transcervical infections were performed to: (1) ensure the establishment of a robust and reliable upper genital tract infection that more closely mimics chronic

infection of the human genital tract with *C. trachomatis* and (2) analyze infection characteristics such as bacterial burden of the upper genital tract.

Within the preliminary experiments, C57Bl/6 mice were infected either intravaginally or transcervically with one of two strains of *C. muridarum*: *C. muridarum* Wild type (WT) , the non-edited natural occurring strain of the bacteria; or *C. muridarum* Δtox, a strain of the bacteria in which the *tc0437*, *tc0438* and *tc0439* ORFs had been deleted from the *C. muridarum* genome. The WT strain of the bacteria served as a control for the experiment, allowing for a comparison of the mutant phenotype of infection to the "normal" phenotype of infection. On day 7 post transcervical or intravaginal infection, genital tract tissue was excised for histopathology, and immunopathology was analyzed externally via anonymized pathology scoring. Vaginal swabs to assess vaginal shedding were collected on days 3, 5 and 7 post intravaginal infection. Additionally, on days 7 and 16 post intravaginal infection only, upper genital tract tissue was harvested and processed for qPCR analysis in order to assess bacterial ascension, the ability of the bacteria to climb to the upper genital tract post infection of the lower genital tract.

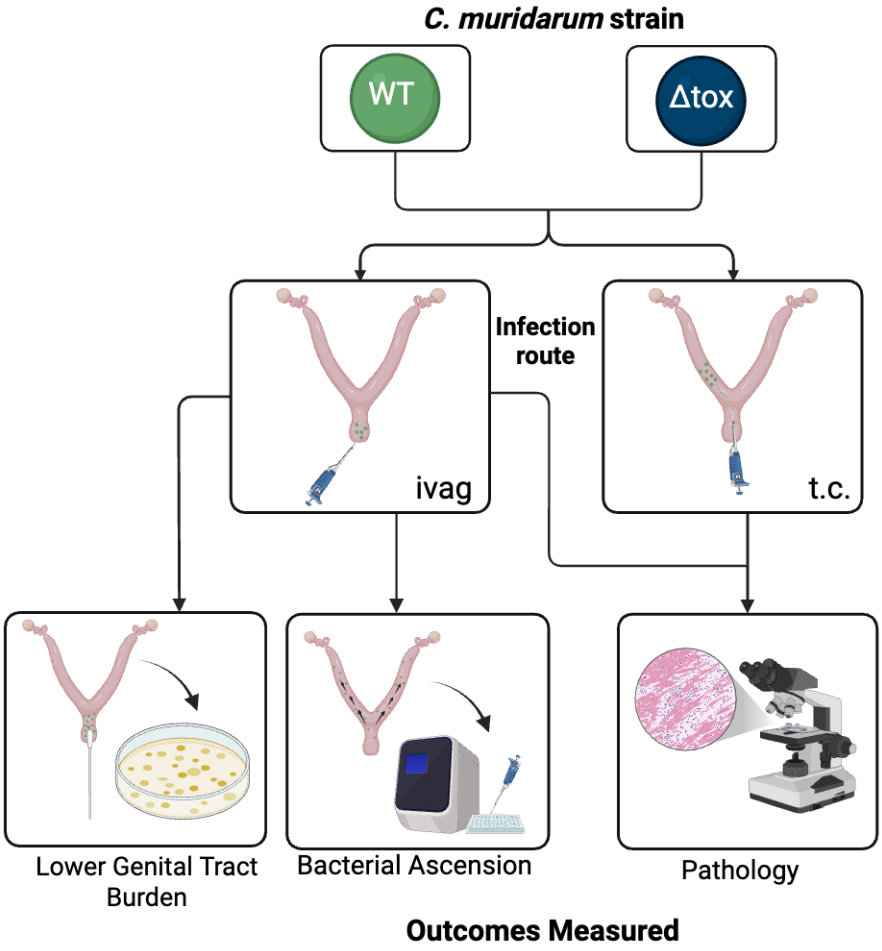

Figure 13. Overview of experimental approach for the preliminary stage of this investigation, including strain type, infection route, and outcome of infection measured. Figure created with BioRender.

The second phase of the study was initiated upon the acquisition of a third strain of the bacteria, *C. muridarum* cistox. The complement of the Δtox strain in which the *tc0437*, *tc0438* and *tc0439* ORFs had been introduced back into the bacteria's genome after their initial deletion, the cistox strain was genetically identical to the WT strain but had been subject to the process of gene editing. Incorporating the complemented strain of the Δtox mutant into the study allowed

us to identify whether our observed results were the product of the mutant phenotype, or if they arose due to genetic manipulation of the bacteria's genome. In the second phase of the study, C57Bl/6 mice were infected either intravaginally or transcervically with one of three strains of *C. muridarum*: *C. muridarum* WT, *C. muridarum* Δtox or *C. muridarum* cistox. Both the WT and cistox strains served as controls for the experiments. On days 3, 7, 11, 15, 21, and 28 post intravaginal infection, vaginal swabs were collected in order to measure vaginal shedding and monitor bacterial burden and persistence in the lower genital tract tissue. Additionally, on day 7 post intravaginal infection, upper genital tracts were excised and processed for qPCR analysis to assess bacterial ascension. Bacterial burden in the upper genital tract was measured by harvesting upper genital tissue on days 3 and 7 post transcervical infection. Lastly, on days 7 and 51 post intravaginal and transcervical infection, entire genital tracts were excised for histopathology, and immunopathology was analyzed internally via anonymized pathology scoring.

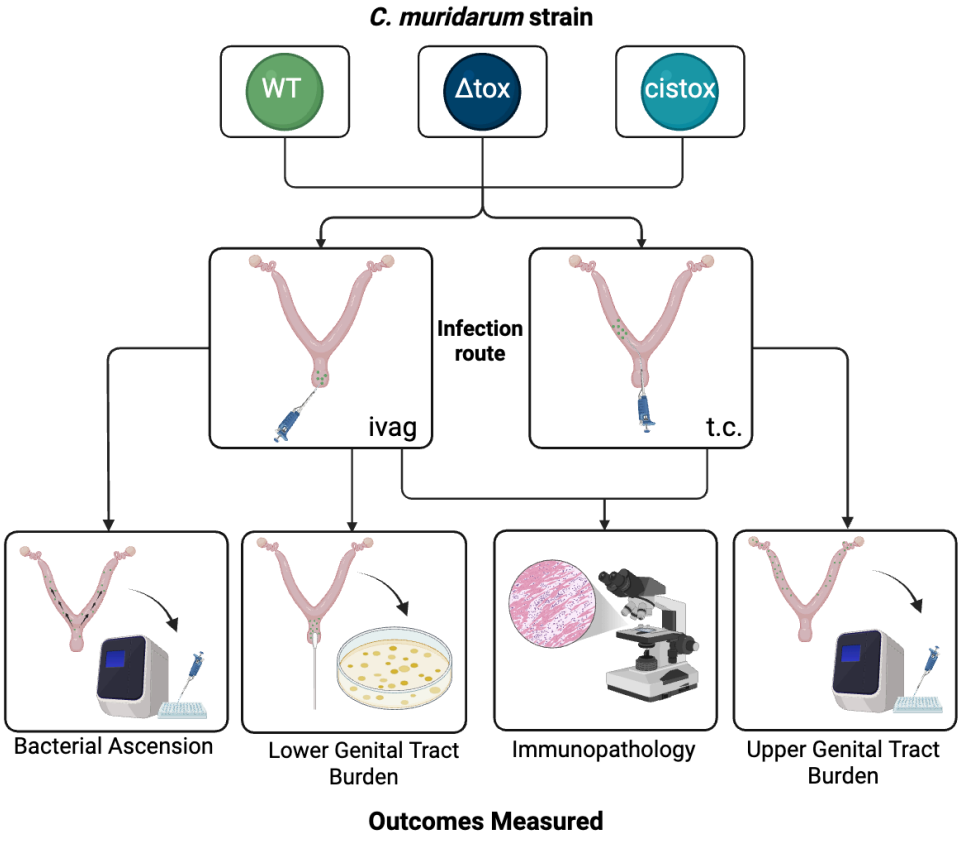

Figure 14. Overview of experimental approach for the secondary stage of this investigation, including strain type, infection route, and outcome of infection measured. Figure created with BioRender.

2. Formal Methods

2.1 Bacterial Strains

Bacterial strains were cultured and genetically modified by our collaborators in the Fields Lab at the University of Kentucky School of Medicine. The three different strains of *C. muridarum* — wild type (WT), Δtox, and cistox — were propagated via cell culture, and infectious elementary bodies were

purified in preparation for mouse genital tract infections. *C. muridarum* Δtox was generated through the deletion of the open reading frames tc0437, tc0438 and tc0439 from the bacterial genome. *C. muridarum* cistox was generated by adding tc0437, tc0438 and tc0439 back into the *C. muridarum* Δtox genome in order to complement the mutant phenotype.

2.2 Mice

All mouse procedures were performed in accordance with protocols approved by the Institutional Animal Care and Use Committees (IACUC) of Mount Holyoke College (BR-66-0624). Female C57Bl/6 mice were purchased from The Jackson Laboratory, housed at Mount Holyoke College, and provided with food and water ad libitum. Mice were 6-8 weeks old when used for intravaginal and transcervical infections.

2.2.1 Genital Tract Infections

Genital tract infections were performed as previously described by Zhang et al. and Gondek et al. (13, 28). Briefly, for both intravaginal and transcervical infections, seven days prior to inoculation (day -7), 5 week old mice were subcutaneously injected with 100 μL of 2.5 mg Depo Medroxyprogesterone Acetate (DMPA) suspended in sterile phosphate-buffered saline (PBS). In preparation for genital tract infections, EBs of the three different bacterial strains were diluted in sterile Sucrose Phosphate Glutamate (SPG) buffer to a

concentration of 10^5 IFUs (Inclusion Forming Units) for the intravaginal inoculations, and 10^6 IFUs for the transcervical inoculations. On day 0, mice were infected with the prepared strains of *C. muridarum* either intravaginally, or transcervically. Prior to intravaginal inoculation, calcium alginate tipped swabs were used to clear the vaginal vault of mice by removing excess mucus from the lower genital tract, as described previously by Morrison et al. (29). Immediately after, mice were challenged with 10^5 IFUs of *C. muridarum* WT, Δtox, or cistox by pipetting 5 µL of the diluted bacterial strains into the vagina of the mouse. Transcervical infections were conducted through the use of a Non-Surgical Embryo Transfer (NSET) device which serves as a thin flexible probe that allows for direct administration of the bacteria into the uterine horns (28). To perform the transcervical inoculation, mice were challenged with 10^6 IFUs of *C. muridarum* WT, Δtox or cistox by pipetting 10 µL of the diluted bacterial strains through the NSET device into the lumenal space of the upper genital tract. See Intravaginal Infection Protocol and Transcervical Infection Protocol in Appendix A.1 and A.2 for further details.

2.2.2 Vaginal Swabs

To both ensure that intravaginal infections were successful and to quantify bacterial burden through the monitoring of vaginal shedding, vaginal swabs were performed at various time points post intravaginal inoculation of mice. Vaginal swab protocols were performed in accordance with the methodology described by

Rixon et al. (30). Prior to performing the swab procedure, calcium alginate micro-tipped swabs were soaked in SPG buffer for 15 minutes. Soaked swabs were then inserted into the vagina of the mouse and rotated 8 times counterclockwise and 8 times clockwise before being placed into 500 µL of SPG. Collected swabs were thoroughly vortexed with 2-3 glass beads for 5 minutes in order to release chlamydial organisms, and then stored at -20˚ C. Bacterial burden analysis of the swabs were performed by the Fields lab at the University of Kentucky by quantifying IFUs. See Appendix A.3 Vaginal Swab Protocol for further details.

2.3 Tissue Processing and Analysis

On days 3, 7, 16, and 51 post infection, mice were sacrificed and genital tracts were excised in order to assess either bacterial burden or immunopathology. The amount of genital tract tissue harvested was dependent on the outcome of infection being measured. For immunopathology analysis, the entire genital tract was harvested, and the tissue was cut approximately 5-6 mm below the cervix. For bacterial burden assessment, genital tract tissue was cut 1-2 mm below the cervix so that only the upper genital tract was harvested. Tissues collected for bacterial burden analysis were homogenized in 2 mL of PBS via mechanical disruption, pipetted into 100 µL aliquots to be analyzed via qPCR and stored at -20˚ C. Tissues collected for immunopathology analysis were fixed in 2 mL of

10% formalin for 24 hours before being transferred to 2 mL of PBS and stored at room temperature.

2.4 Quantifying Bacterial Burden by quantitative PCR

Genital tract homogenates were assessed for *Chlamydia* burden via a quantitative PCR (qPCR) assay that had been previously shown to accurately reflect the levels of *Chlamydia* inclusion forming units (IFUs). To acquire a DNA template for the qPCR assay, tissue was digested and genomic DNA was extracted from the 100 µL homogenate aliquots using the DNeasy Blood and Tissue Kit (Qiagen). *Chlamydia* 16S specific primers and probe were designed and generated through Integrated DNA Technologies (IDT) and were as follows:

16S forward primer sequence: 5’ - GGA GGC TGC AGT CGA GAA TCT - 3’
16S reverse primer sequence: 5’ - TTA CAA CCC TAG AGC CTT CAT CAC A - 3’
16S probe sequence: 5’ - / 56-FAM / TCG TCA GAC TTC CGT CCA TTG CGA / 36-TAMSp / - 3’

Host mouse GAPDH DNA was quantitated for normalization of 16S DNA. Mouse GAPDH specific primers and probe were generated from TaqMan® Rodent GAPDH Control Reagents (Applied Biosystems). *Chlamydia* 16S DNA and Host Mouse GAPDH DNA were amplified and quantified from extracted

homogenate DNA using an Aria MX Real-Time PCR system (Agilent). The ratio of *Chlamydia* 16S DNA to mouse GAPDH DNA was then calculated using standard curves generated from known amounts of purified *Chlamydia* or mouse DNA. See Appendix A.4 DNA extraction protocol and Appendix A.5 qPCR protocol for further details.

2.5 Immunopathology Analysis

2.5.1 Assessing Gross Pathology

Prior to fixing tissue in formalin for immunopathology analysis, the gross pathology, or macroscopic state of the excised genital tract tissue was assessed to determine disease severity. Tissue was qualitatively assessed for the presence of hydrosalpinx, evident as clear glass-like bulbs of fluid at the end of the uterine horns, and uterine horn dilation, evident as swelling and distention of the horn tissue. Presence of hydrosalpinx in individual oviducts was quantified and compared across mice infected with the different strains. Photos of genital tracts were obtained through imaging of the tissue immediately upon excision.

2.5.2 Assessing Immunopathology

Tissues fixed in formalin for histopathology analysis were submitted to the Rodent Histopathology Core Facility at Harvard Medical School. Genital tracts were paraffin embedded, stained with hematoxylin and eosin (H&E), and

sectioned to a thickness of 4-5 μm to allow for visualization of the tissue by microscopy.

For the preliminary stage of this investigation, immunopathology was assessed externally by a pathologist at the Rodent Histopathology Core Facility at Harvard medical school. Severity scoring was assigned based on how much of the tissue was affected by the presence of pathology phenotypes including: fibrosis, edema, epithelial/membrane thickening and/or degeneration, luminal/tissue cellular infiltration, and increased vascularity. Scores assigned to the tissue ranged from 0 (no pathology); 1 (mild/rare pathology, less than 1/3 of tissue affected); 2 (moderate/ multifocal pathology, between 1/3–2/3 of tissue affected); to 3 (severe/coalescing pathology, greater than 2/3 of tissue affected). A more comprehensive outline of this external pathology scoring was described in a previous publication by the Lijek lab (5).

For the secondary stage of this study, immunopathology was analyzed internally by a team of individuals in the Lijek lab who developed a novel scoring system that was both in accordance with the histopathology literature and best reflected the diversity in pathology upon *C. muridarum* infection (31, 32, 33). Immunopathology of the upper genital tract was assessed via their anonymized semi quantitative scoring system in which tissues were assigned severity scores based on the prevalence of pathology phenotypes associated with human female upper genital tract infection with *C. trachomatis*. Anatomic sites (uterine horn, oviducts, ovaries) were assessed independently for both cellular infiltration

(neutrophils, lymphocytes) and presence of edema or dilation (swelling). After acute infection in which tissue was excised 7 days post infection, anatomic sites were assigned general pathology scores. After chronic infection in which pathology was more robust and varied amongst mice each anatomical site was assigned two scores, one representing edema/dilation, and one representing cellular infiltration. Each anatomical site was scored via a unique range that was developed to reflect the differences in pathology witnessed during infection with the different *C. muridarum* strains, and a comprehensive outline of this scoring system can be found in Appendix B Pathology Scoring Guidelines.

Representative images of the three anatomical sites assessed for pathology were taken for each condition at 10x magnification on a Nikon Eclipse 50i using brightfield microscopy and a PixeLink camera. Both ImageJ and Cellsens were used to stitch individual images together to generate figures presenting whole ovaries, whole oviducts, and partial sections of uterine horns.

2.6 Statistical Analysis

Statistical analysis was performed using Prism (GraphPad). When comparing two conditions, differences between groups were determined using an unpaired Student's T-test and a P value of < 0.05 was considered significant. Comparison of three conditions was performed by using one-way analysis of variance (ANOVA), with a P value of < 0.05 again being considered significant. All bar graphs are shown as mean ± SEM, where **** $P < 0.0001$, *** $P < 0.001$,

** $P < 0.01$, * $P < 0.05$, and N.S. indicates not significant by unpaired student's t-test. Amplification and melt curves were generated using Agilent Aria Software v1.5

RESULTS

1. Preliminary Stage Results

1.1 The contribution of chlamydial putative virulence factors to *C. muridarum* pathogenesis in vivo can be dissected using a genetic approach

Previous studies assessing the function of the *Chlamydia* putative virulence factors *CT166* and *tc0437-0439* have taken different approaches in order to discern whether or not these open reading frames contribute to chlamydial pathogenesis. In the Lijek lab, our previous vaccine study had coupled an immunological approach to a mouse model with the purpose of identifying whether or not antibody mediated inhibition of CT166 impacted the development of immunopathology. In contrast, studies by the Fields lab instead took a genetic approach, using mutant strains of the bacteria in which *tc0437-0439* had been deleted to determine the impact of these ORFs in vitro by performing cell culture studies. Our research combines these two strategies, taking a genetic approach but using an in vivo model in order to address these same questions. As this approach has yet to be evaluated thus far, for the means of our study it was essential to conduct a series of preliminary studies to first determine whether or not taking a genetic approach via a mouse model was a feasible and effective method of assessing the virulence of these open reading frames.

1.2 Infection with Δtox results in reduced immunopathology of the upper genital tract

To evaluate this approach, we first investigated whether or not there was a difference in infection phenotype upon challenge with *C. muridarum* Δtox versus *C. muridarum* WT. Mice were challenged transcervically or intravaginally with the two different strains of the bacteria, and immunopathology was assessed on day 7 post infection.

A

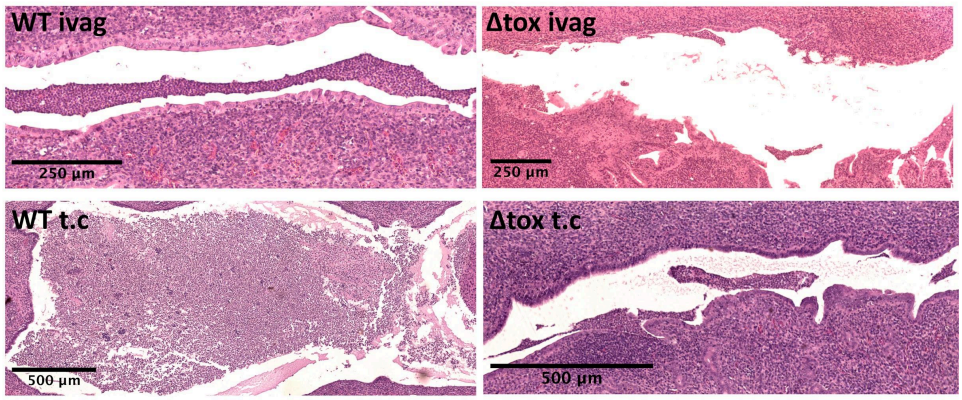

B

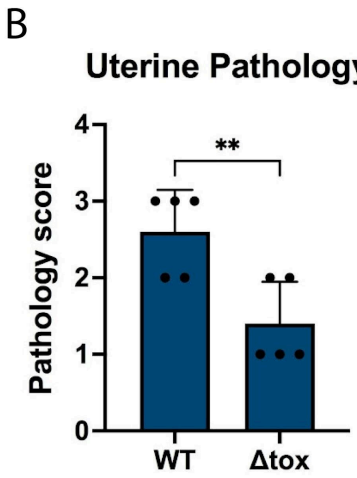

Figure 15. Deletion of *tc0437-0439* from the *C. muridarum* genome significantly reduces neutrophil infiltration into the uterine horns during both transcervical and intravaginal infection. H&E stained mouse uteri (A) 7 days post transcervical (t.c.) or intravaginal (ivag) infection with *C. muridarum* WT or Δtox. Uterine pathology scores of transcervical challenge (B) were assessed externally by the Harvard Rodent Histopathology Core under anonymized conditions. Pathology was scored on a 0-4 scale, where a higher score indicated increased immune cell invasion into the lumenal space of the uterine horns. Significance was determined via a Mann-Whitney U test with a p-value of <0.05

A

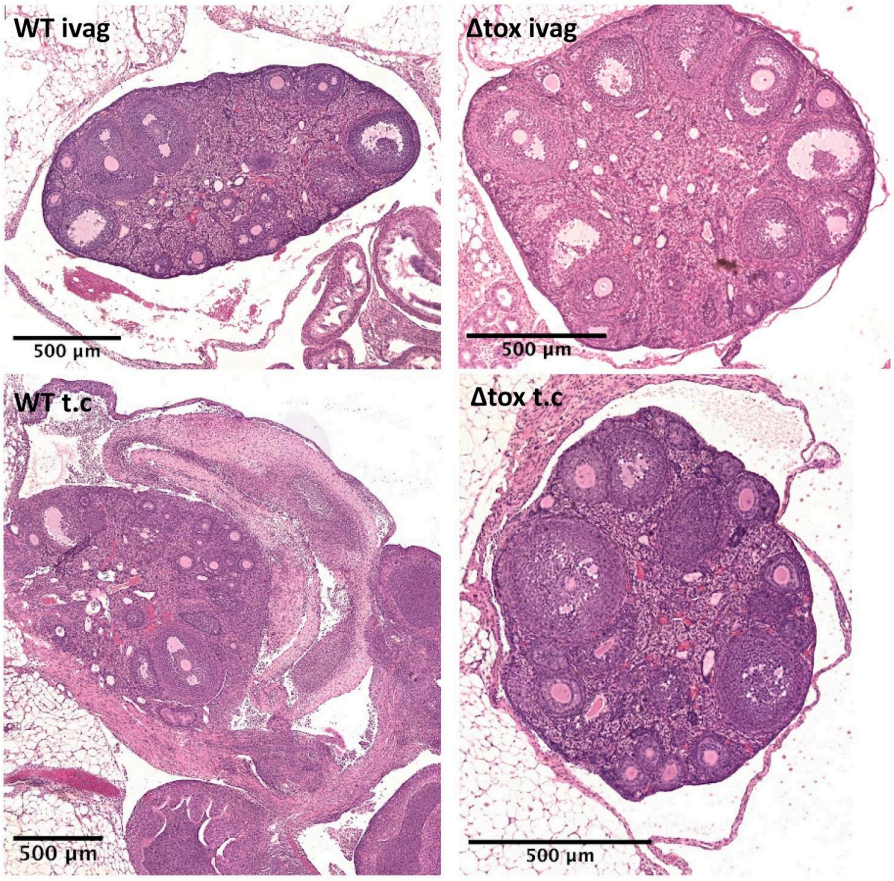
WT ivag
Δtox ivag
WT t.c
Δtox t.c
500 µm
500 µm
500 µm
500 µm

B

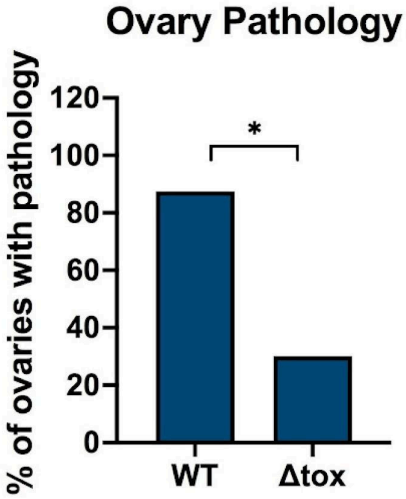
Ovary Pathology
% of ovaries with pathology
120
100
80
60
40
20
0
*
WT
Δtox

Figure 16. Δtox significantly ameliorates immunopathology of the ovaries and oviducts during both transcervical and intravaginal infection. H&E stained mouse ovaries 7 days (A) post transcervical (t.c.) or intravaginal (ivag) infection with *C. muridarum* WT or Δtox. Pathology presence in the ovaries was determined by assessing ovarian membrane separation and immune cell infiltration into the ovary and oviducts. % pathology (B) was quantified by dividing the number of ovaries with pathology over the total number of ovaries infected with each respective strain. Significance was determined via a chi-squared test.

Upon qualitative examination of the tissue, there was a clear difference in immunopathology of both the uterine horns (Figure 15A) and ovaries (Figure 16A) in mice challenged with the two different strains. Mice infected with Δtox had strikingly lower neutrophil infiltration into the uterine horns, and exhibited less ovary edema and oviduct inflammation. This was marked by reduced thickening and separation of the ovarian membrane, and diminished swelling of the oviduct tissue. This qualitative assessment of the tissue was mirrored by our quantitative analysis of the presence of pathology in the tissue. Pathology scores of the uterine horns (Figure 15B) and % pathology of the ovaries (Figure 16B) were significantly lower in mice infected with the Δtox strain of the bacteria compared to the WT strain, mirroring what we witnessed through the microscope. Taken together, these results indicate that infection with the Δtox strain results in a different pathology phenotype compared to the WT strain, and that this phenotype is marked by a reduction in immunopathology of the upper genital tract.

Also notable from these results was that, while both intravaginal and transcervical infection resulted in a difference in pathology between the Δtox and WT strains, the robustness of this pathology varied depending on the route of inoculation. When mice were infected transcervically, there was a strong, robust response to the bacteria. Uterine horns were slightly more dilated, there was a higher presence of neutrophils in the tissue, and the ovaries and oviducts were incredibly swollen and inflamed (Figure 16A WT t.c.). In comparison, while mice infected intravaginally still displayed pathology, there was less neutrophil infiltration into the uterine horns, and inflammation in the ovaries was strikingly reduced, with only mild ovarian membrane separation and neutrophil presence. Of these results, the robust response of the transcervical infection more closely mimics what is seen in human tissue during *Chlamydia* infection.

1.3 Bacterial Burden

Chlamydia infection is defined by two central features: the ability of the bacteria to establish infection, and the pathology that the bacteria elicits upon infection. Thus, in addition to assessing the host response to the bacteria, immunopathology, we performed a second set of preliminary experiments that were instead targeted towards determining if this approach was a feasible method to evaluate whether or not *tc0437-0439* impacted the ability of the bacteria to infect host tissue.

1.3.1 Δtox successfully infects the lower genital tract relative to the WT strain

During *Chlamydia* infection in humans, the bacteria initially infects the tissue of the lower genital tract, the vagina and the cervix. This is mimicked in a mouse model via the intravaginal route of inoculation, in which the bacteria is deposited into the lower genital tract of the mouse. Both in humans and in mice, if the initial infection of the lower genital tract (LGT) is not successful, the bacteria cannot reach the upper genital tract and establish a robust infection. Vaginal shedding serves as a means of measuring *Chlamydia* burden in the LGT of mice and monitoring how this burden changes throughout the time course of an infection. It is therefore indicative of the ability of the bacteria to both infect the LGT and persist within the tissue until clearance.

To monitor LGT burden, we infected mice intravaginally with either the Δtox or WT strain of the bacteria, and took vaginal swabs on days 3, 5, and 7 post infection as a means of collecting vaginal shedding. The amount of bacteria present in the lower genital tract was quantified by measuring *Chlamydia* Inclusion Forming Units (IFUs) from the swabs. The vaginal swab time points were chosen to reflect when the bacteria is likely still present in the LGT, as it often ascends up the reproductive tract at approximately day 7 - day 10 post infection (34).

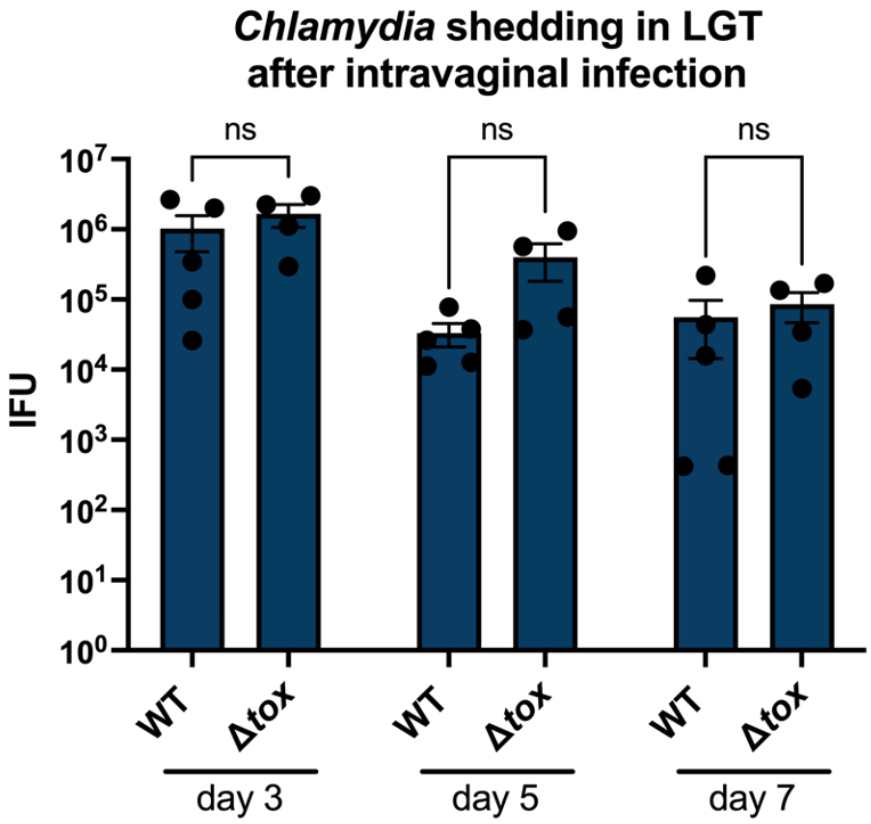

Figure 17. Absence of *tc0437-0439* from the *C. muridarum* genome does not significantly impact vaginal shedding upon intravaginal infection. Vaginal shedding of *Chlamydia* measured on days 3, 5, and 7 post intravaginal infection. Shedding was collected via vaginal swabs, and IFUs of those swabs were quantified by the Fields lab at the University of Kentucky. Non significance was determined by two-way ANOVA followed by Šídák's multiple comparisons test.

At each of the three timepoints, mice infected with the Δtox strain exhibited no significant difference in vaginal shedding compared to mice infected with the WT strain (Figure 17). *Chlamydia* IFUs in the LGT were highest on day 3 post infection, and decreased slightly as the infection progressed, which is to be

expected as the bacteria leaves the lower genital tract to ascend up the reproductive tissue throughout the course of infection. This slight decrease in LGT burden as the infection progressed was consistent across the Δtox and WT strains. Notably, one mouse infected with Δtox did not exhibit any vaginal shedding of the bacteria despite being infected, and thus was not included in the figure above as no IFU count could be quantified. This outlier is likely a result of the unreliability of the intravaginal infection route, and is not representative of the mutant phenotype of the Δtox strain. As vaginal shedding is indicative of bacterial burden in the lower genital tract, these results suggest that we are able to both quantify LGT burden via vaginal swab analysis, and that the Δtox strain of the bacteria is able to establish infection in the lower genital tract as effectively as the WT strain is.

1.3.2 Δtox is capable of ascending to the upper genital tract to the same extent as the WT strain

After *Chlamydia* invades the lower genital tract, the bacteria ascends past the cervix and makes its way to the upper genital tract (UGT). This ascension is believed to be critical for the bacteria to establish infection in the UGT and induce immunopathology (35). Having identified in the previous experiment that there is no difference in the ability of *C. muridarum* Δtox and WT to infect the lower genital tract, the next step of our study was to determine whether or not the next phase of infection, ascension, was impacted by deleting *tc0437-0439* from the *C.*

muridarum genome. To explore this, mice were challenged intravaginally with either *C. muridarum* Δtox or *C. muridarum* WT, and upper genital tracts were harvested on day 16 post infection for qPCR analysis. It was critical that only the upper genital tracts were collected, to ensure that ascension, and not lower genital tract burden, was being measured.

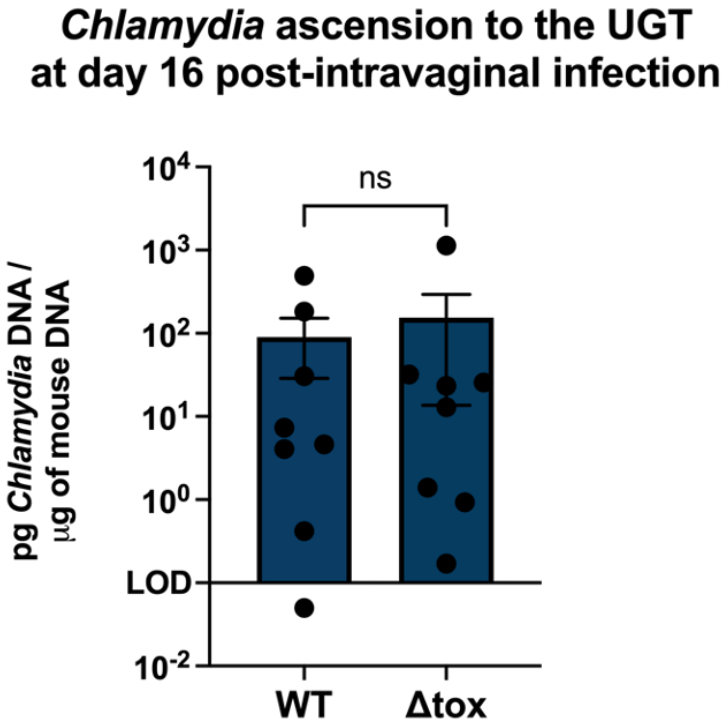

Figure 18. Absence of *tc0437-0439* does not impact *Chlamydia* ascension in vivo. Bacterial ascension from the lower genital tract to the upper genital tract of mice infected intravaginally with either the Δtox or WT strain of *C. muridarum*. Upper genital tracts (UGT) were excised on day 16 post infection, and ascension was quantified via qPCR analysis of DNA extracted from UGT homogenates. Non significance was determined by an unpaired t-test.

When comparing the data collected across the two strains, there was no significant difference in *Chlamydia* ascension in mice infected with Δtox versus mice infected with the WT strain. As evident in Figure 18, data for both strains was highly variable, falling within a range of approximately 10^{-1} to 10^{3} pg *Chlamydia* DNA/ µg of mouse DNA, a 4 times log_{10} fold change. This variability, although striking, was what we expected to see when observing *Chlamydia* ascension.

In humans, not every *Chlamydia* infection results in severe pathology and the development of disease sequelae. The reason for this being that even after infection of the vagina and cervix, the bacteria is not always capable of ascending to the upper genital tract and establishing an infection in the uterus and ovaries. This strong variability in ascension for both the Δtox and WT strain suggests that the transcervical inoculation method, which bypasses the need for bacterial ascension by depositing the bacteria directly into the upper genital tract, may be the most effective method to study how the bacteria induces a disease state. This echoes the results of our preliminary pathology experiment, which indicated that transcervical challenge resulted in a more robust infection of the upper genital tract tissue.

The results of this preliminary experiment suggest three critical concepts: (1) we are able to quantify bacterial ascension in mice via qPCR analysis (2) the ascension of *Chlamydia* is not impacted by the absence of putative virulence factors *tc0437-0439*, and (3) transcervical inoculation offers the most reliable

route of infection in order to observe how these open reading frames impact robust infection.

1.4 Summary of Preliminary Results

Taken together this preliminary study provides evidence that deletion of the putative virulence factors *tc0437-0439* from the *C.muridarum* genome reduces immunopathology of the UGT, but does not impact the ability of the bacteria to infect the lower genital tract or ascend to the upper genital tract during the course of infection. These results were extremely promising, and strongly suggested the need to both further dissect the infection phenotype elicited by the Δtox strain and further evaluate the ability of the bacteria to infect the genital tract, particularly in regards to the last stage of *Chlamydia* infection, invasion of the upper genital tract. Thus, the preliminary phase of this study achieved three things: it validated our methodology in regards to infection mechanism and data collection, it established that using a genetic approach in vivo was an effective means of addressing the key questions of the study, and it justified the need for further, more extensive research into this subject using this same approach.

2. Secondary Stage Results

To address this need for more extensive research, we transitioned into the second phase of the study which, similar to the preliminary phase, again assessed aspects of immunopathology and bacterial burden during infection with different

strains of *C. muridarum*, but had key differences in comparison to the first phase. In particular, this second set of experiments examined infection at a later time point, focused on the transcervical route to assess pathology, and incorporated the complemented strain of Δtox, known as cistox, into the study. We chose to focus on the transcervical route of infection as the preliminary studies highlighted that this was the most reliable and accurate method of mimicking human *Chlamydia* infection. The complemented strain served as both a second control and internal validation of our findings, as it was a means of identifying whether or not our observed results were the product of specifically deleting *tc0437-0439*, or the product of genetic manipulation of the bacteria's genome in general.

2.1 Assessment of Bacterial Burden

2.1.1 Δtox does not persist in the lower genital tract to the same extent as the control strains

Our preliminary experiment assessing lower genital tract burden identified that the Δtox strain was able to successfully infect the LGT. However, as we only collected shedding during the early time points of infection, this data does not indicate whether or not the Δtox strain is capable of persisting within the LGT tissue. The ability of the bacteria to remain viable and persist within the host tissue for extended periods of time has been linked to the development of disease sequelae in humans (36). Thus, to gain a stronger idea of how the Δtox strain persists within the LGT tissue, we performed a repeat experiment that monitored

vaginal shedding up until the later stages of infection. Mice were infected intravaginally with either the Δtox, WT, or cistox strains, and vaginal swabs were collected on days 3, 7, 11, 15, 21, and 28. Vaginal shedding was quantified via IFU analysis by the Fields lab at the University of Kentucky.

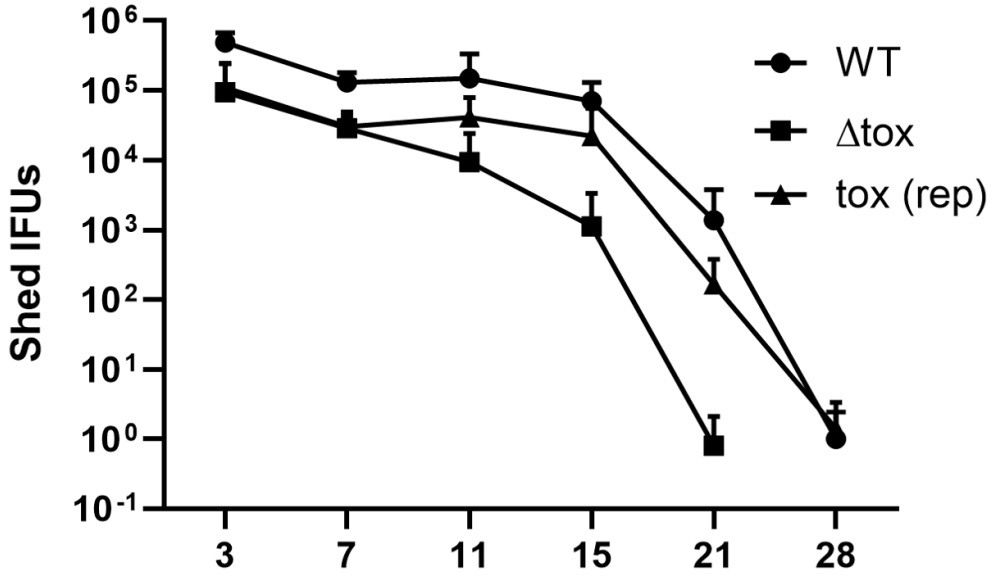

Figure 19. The Δtox strain of *C. muridarum* is cleared from the lower genital tract earlier than the WT and cistox strains. Vaginal shedding of *Chlamydia* measured on days 3, 7, 11, 15, 21, and 28 post intravaginal infection with the WT, Δtox, or cistox (tox (rep)) strains of the bacteria. Shedding was collected via vaginal swabs, and IFUs were quantified by the Fields lab at the University of Kentucky. Differences in IFUs between mice infected with the Δtox strain versus mice infected with the two controls (WT, cistox) on days 21 and 28 post infection were found to be significant via two-way ANOVA.

The shedding data collected during the early stages of infection, at days 3 and 7, match that of our preliminary results, as there is no significant difference in IFUs between the Δtox strain or either of the controls at these timepoints (Figure

19). This validates our earlier finding that the Δtox strain successfully establishes infection in the lower genital tract. However, beginning at day 11 post infection, the amount of Δtox strain in the LGT starts to vary compared to the WT and cistox strains. While IFUs of the WT and cistox strain remain relatively constant between days 7 and 15, IFUs of the Δtox strain noticeably decrease during this time. This difference becomes more pronounced as the course of infection continues, as the Δtox strain is cleared by Day 21 post infection, while both the WT and cistox strains are only cleared on Day 28 post infection, an entire week later. This suggests that the Δtox strain does not persist in the LGT as long as the WT and cistox strains do, and is cleared from the LGT tissue earlier on in infection.

2.1.2 There is no difference in *Chlamydia* ascension between the WT, cistox, and Δtox strains

The results of our earlier ascension experiment were highly variable, and while this is consistent with what we see during human infection, to ensure that our results were accurate, we repeated our assessment of ascension, this time with the cistox strain as well. Mice were challenged intravaginally with either the WT, Δtox, or cistox strain and upper genital tracts were excised on day 7 post infection. Ascension was assessed on day 7 in this repeat experiment as previous studies had noted the presence of *Chlamydia* in the upper genital tract at this earlier time point already (34).

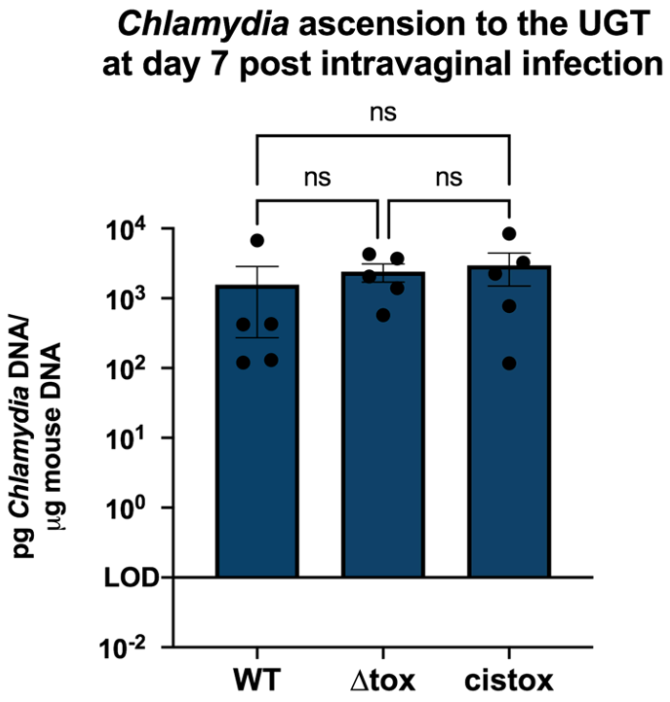

Figure 20. Infection with Δtox does not impact the ability of *Chlamydia* to ascend relative to the controls. Bacterial ascension from the lower genital tract to the upper genital tract of mice infected intravaginally with *C. muridarum* Δtox, WT, or cistox. Upper genital tracts (UGT) were excised on day 7 post infection, and ascension was quantified via qPCR analysis of DNA extracted from UGT homogenates. Non significance was determined by a one-way ANOVA followed by a Tukey's multiple comparisons test.

Consistent with our preliminary experiment, there was no significant difference in *Chlamydia* ascension between mice infected with the Δtox strain versus mice infected with the WT and cistox strains (Figure 20). The data was not quite as spread as our earlier results, however was still variable, falling between 10^2 to 10^4 pg *Chlamydia* DNA/ µg of mouse DNA, a 2 times log_{10} fold change. This moderate variability again mirrors human infection, and serves as an

indication that the transcervical route of inoculation is the most effective route to assess robust upper genital tract infection. As these ascension results mirror our findings from the preliminary experiment, they strongly suggest that deletion of *tc0437-0439* from the *C. muridarum* genome does not impact the ability of the bacteria to ascend during *Chlamydia* infection.

2.1.3 Δtox successfully infects the upper genital tract relative to the WT and cistox strains

Having identified that the Δtox strain was able to successfully infect the lower genital tract and ascend, it was next necessary to evaluate whether or not these putative virulence factors impacted the final stage of *Chlamydia* infection: invasion of the upper genital tract (UGT). To measure the ability of the Δtox strain to directly infect the UGT, it was critical to transcervically inoculate mice, so that the first two stages of *Chlamydia* infection could be bypassed. Thus, to assess UGT bacterial burden we challenged mice transcervically with *C. muridarum* Δtox, WT, or cistox, and on day 3 and day 7 post infection excised the genital tract tissue for DNA extraction and qPCR analysis.

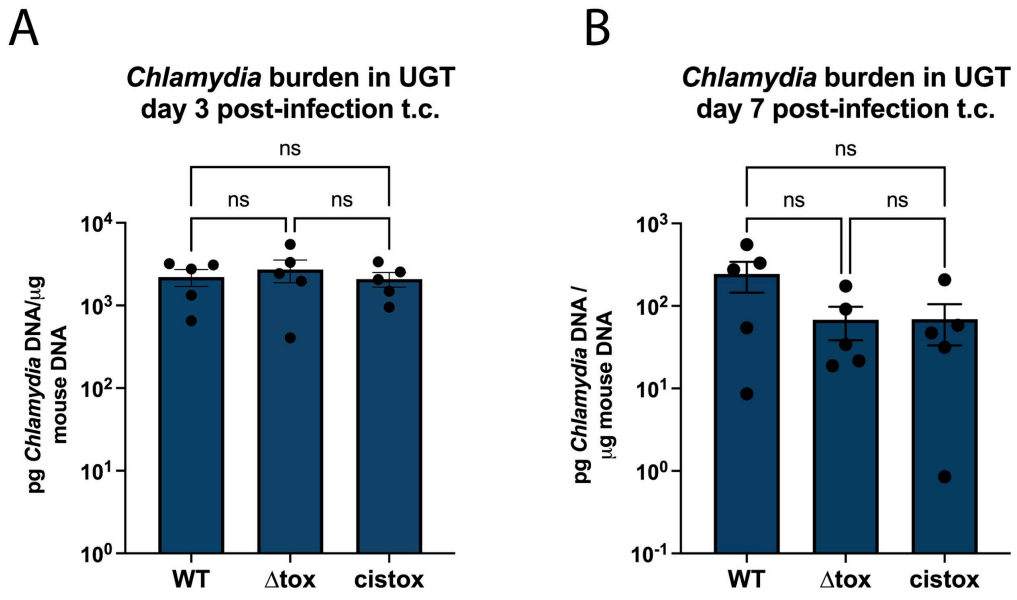

Figure 21. Upper genital tract *Chlamydia* burden does not vary between mice infected with either the Δtox, cistox, or WT strain of *C. muridarum*. Upper genital tracts were harvested on both day 3 and day 7 post transcervical challenge, and bacterial burden was quantified via qPCR analysis of DNA extracted from UGT homogenates. Non significance was determined by a one-way ANOVA followed by a Tukey's multiple comparisons test.

Similar to our previous burden experiments, there was no significant difference in bacterial burden of the upper genital tract of mice infected with either the Δtox, WT, or cistox strains at either time point (Figure 21). On day 3 post infection, burden was relatively high for all three strains. There was some slight variability in the data at this time point, but burden remained consistently high both within strains and across strains. In comparison, on day 7 the amount of *Chlamydia* in the UGT after infection with Δtox, WT, and cistox appeared to decrease, and the data became more variable. Both the decrease and variability in

burden align with what we expect to see during infection of the upper genital tract. Previous studies using mouse models to monitor the protective immune response to *Chlamydia* have identified that CD4+ T cells begin to clear the infection from the upper genital tract approximately 7 days after transcervical infection (28). Clearance of the bacteria at this time point would result in a slight decrease in UGT burden, which is what we see on day 7 for the Δtox, WT, and cistox strain. It would also account for the variability within our data, as the rate at which infection clearance occurs can vary across organisms, and thus some mice may have mounted a protective immune response faster than others. As UGT burden on both day 3 and day 7 remained consistent across all three strains, these results suggest that the Δtox strain is able to establish an upper genital tract infection as effectively as the WT and cistox strains.

2.2. Pathology Analysis

The preliminary immunopathology results strongly suggested that the Δtox and WT strains elicited different infection phenotypes, with the Δtox strain resulting in reduced immunopathology. However, the extent to which this reduction impacted different anatomical features of the upper genital tract tissue and how the Δtox immunopathology phenotype differed from the cistox phenotype, remained unclear. To address this gap in our knowledge, a pathology crew team in the lab developed an anonymized pathology scoring system in which they analyzed the presence of immunopathology within the tissue. The criteria for

assessing the tissue was dependent upon the route of infection (intravaginal vs transcervical), the anatomy of the tissue (uterine horn, ovary, oviduct), the type of pathology (cellular infiltration, edema) and the time point of the tissue analysis (acute vs chronic infection). Their scoring protocol was rigorously developed and is highly complex, and thus a more detailed breakdown of their scoring system can be found in the methods and Appendix B.

To dissect how immunopathology of the uterine horns, ovaries, and oviducts differs across infection with the three different strains, we challenged mice transcervically with *C. muridarum* Δtox, WT, or cistox. On days 7 and 51 post infection, genital tracts were excised to be analyzed both qualitatively and quantitatively for immunopathology, using microscopy analysis and the novel in-house pathology scoring system. The transcervical route of infection was used to inoculate the mice as both the preliminary immunopathology and burden results indicated that this was the most reliable method to ensure robust infection of the upper genital tract.

For this particular set of experiments, we looked at two different time points, day 7 and day 51. Day 7 served as a model of acute infection, the beginning stages of *Chlamydia* invasion of the UGT when the bacteria begins to induce immunopathology. In comparison, day 51 acted as a model of chronic infection, when immunopathology has persisted in the tissue for an extensive period of time and thus has begun to lead to the development of sequelae.

Exploring how the bacteria impacts both acute and chronic inflammation offers insight into what role the putative virulence factors may play in inducing immunopathology of the upper genital tract.

2.2.1 Oviduct histopathology is reduced upon acute Δtox infection

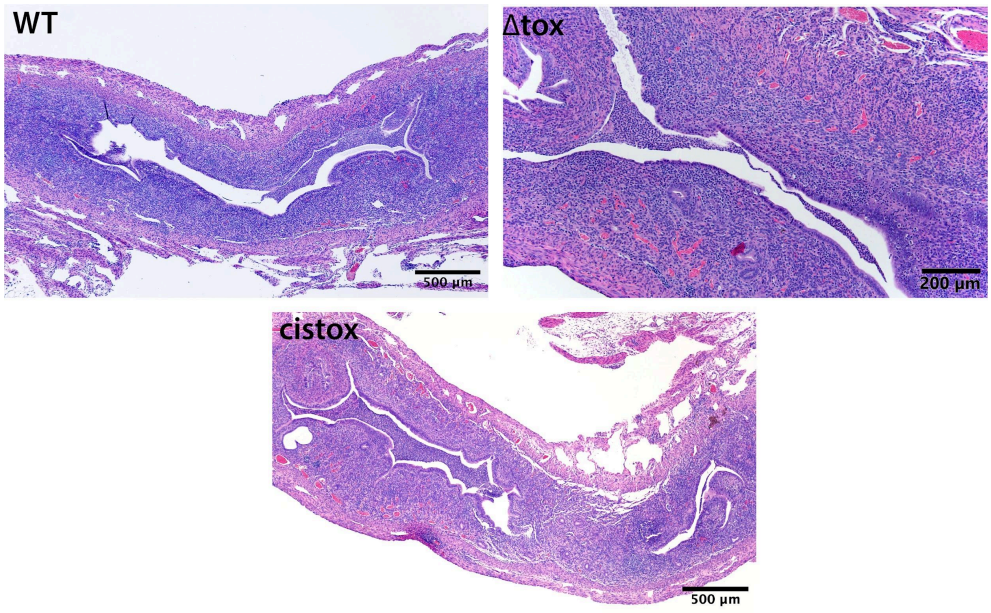

Figure 22. Δtox does not reduce uterine horn pathology during acute upper genital tract infection. H&E stained mouse uteri post transcervical infection with the WT, Δtox, or cistox strains of *C. muridarum*. Genital tracts were excised on Day 7 post infection, and sectioned and stained by the Harvard Rodent Histopathology core. Images were photographed via a Pixelink camera on a Nikon Eclipse 50i scope. Images were stitched together via cellSens imaging software and scale bars were added via ImageJ.

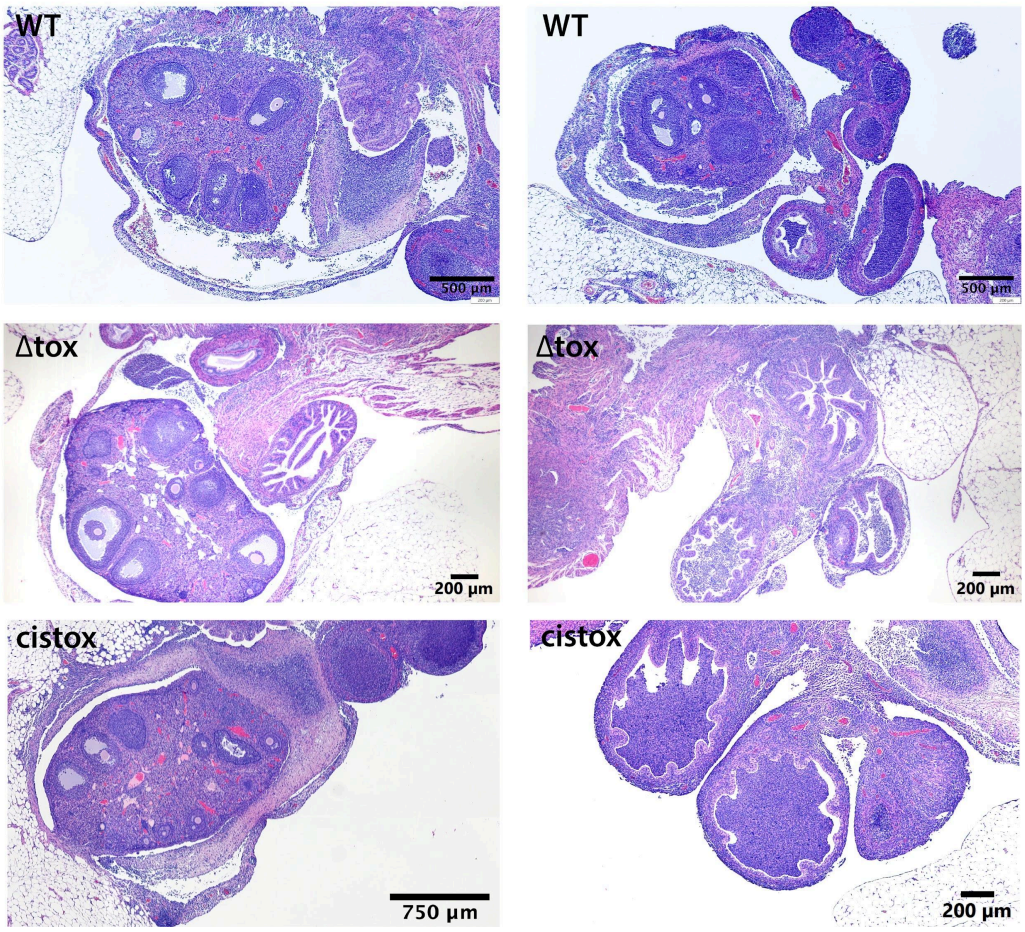

Figure 23. Δtox results in reduced oviduct immunopathology during acute upper genital tract infection. H&E stained mouse ovaries and oviducts post transcervical infection with the WT, Δtox, or cistox strains of *C. muridarum*. Genital tracts were excised on Day 7 post infection, and sectioned and stained by the Harvard Rodent Histopathology core. Images were photographed via a Pixelink camera on a Nikon Eclipse 50i scope. Images were stitched together via cellSens imaging software and scale bars were added via ImageJ.

Upon qualitative assessment of the tissue, there were no notable differences in immunopathology of the uterine horns between mice infected with the three different strains. Infection with each strain resulted in neutrophil

infiltration into the lumen, and minimal uterine dilation or swelling (Figure 22). Similarly, acute infection of the ovaries did not differ largely across the three strains. Mice infected with the WT and cistox strain had slightly thicker ovarian membranes, but there were similar levels of ovarian membrane separation and ovarian edema upon infection with Δtox, WT, and cistox (Figure 23). What was noticeably different across the three strains, was immunopathology of the oviducts. In mice infected with the WT and cistox strains, the oviducts were filled with neutrophils, and appeared swollen and inflamed. In comparison, mice infected with the Δtox strain had minimal or no neutrophil infiltration in the oviducts, and the tissue did not appear swollen.

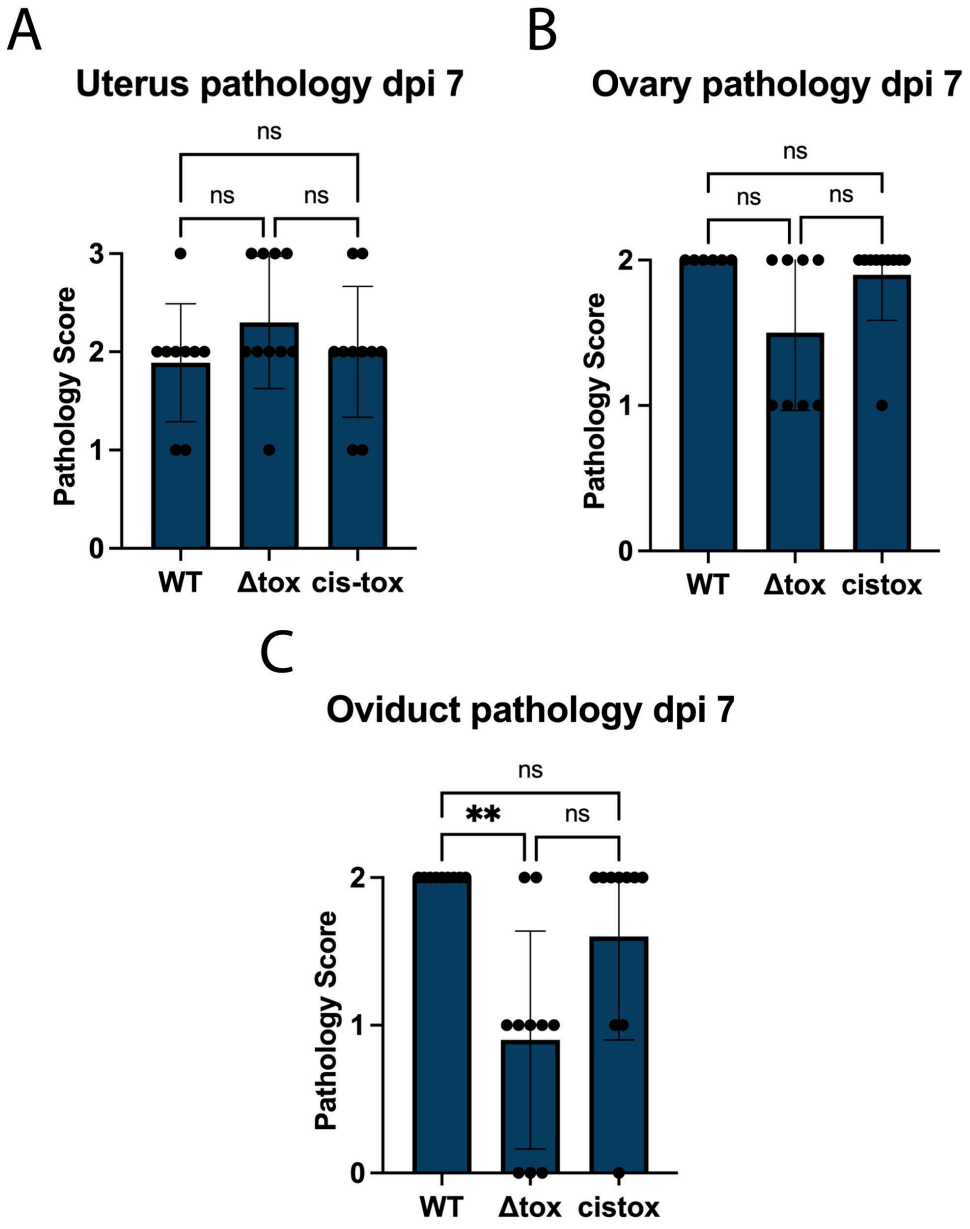

Figure 24. General pathology scores of upper genital tract tissue indicate significantly reduced oviduct immunopathology during acute Δtox infection. General pathology was anonymized and determined by evaluating cellular infiltration and edema of the tissue. Pathology of the ovaries and oviducts was assessed on a 0-2 scale, while pathology of the uterine horns was assessed on a 0-3 scale. The higher the score, the higher the presence of neutrophils and swelling within the tissue. Significance was determined by the Kruskal-Wallis test using a p-value of < 0.01, followed by Dunn's multiple comparisons test.

Our qualitative assessment of the tissue was consistent with the pathology scoring analysis carried out by the pathology crew in the lab. There were no significant differences in either uterine horn pathology (Figure 24A) or ovary pathology (Figure 24B) between mice infected with the three strains. However, mice infected with Δtox displayed significantly reduced oviduct pathology in comparison to mice infected with the WT strain (Figure 24C). Collectively, the qualitative and quantitative assessment of these results suggest that infection with Δtox results in reduced immunopathology of the oviduct during acute *Chlamydia* infection.

2.2.2 Δtox ameliorates the presence of gross pathology during chronic infection

During chronic *Chlamydia* infection, immunopathology in the upper genital tract persists for an extended length of time, and therefore often leads to the development of disease sequelae. These sequelae can be well characterized at the cellular level via histopathology analysis, but are often noticeable to the naked eye. Gross pathology is the macroscopic assessment of the tissue, and is a technique that can often implicate a disease state without requiring staining and microscopy. Hydrosalpinx, the severe swelling of the oviducts, is a common consequence of robust chronic *Chlamydia* infection. It is highly visible at the gross pathology level, appearing as a bright clear bulb of fluid on the end of the

uterine horns, giving the oviduct a swollen “glass” appearance.

Having witnessed a significant difference in oviduct immunopathology during acute infection, identifying whether or not there was a difference in hydrosalpinx upon infection with the different strains during chronic infection was of great interest to our research. Thus, upon excising the genital tracts on day 51 post infection, we began by assessing gross pathology of the tissue, particularly looking at whether or not “glass” oviducts, and therefore hydrosalpinx, were present for all three strains. .

A

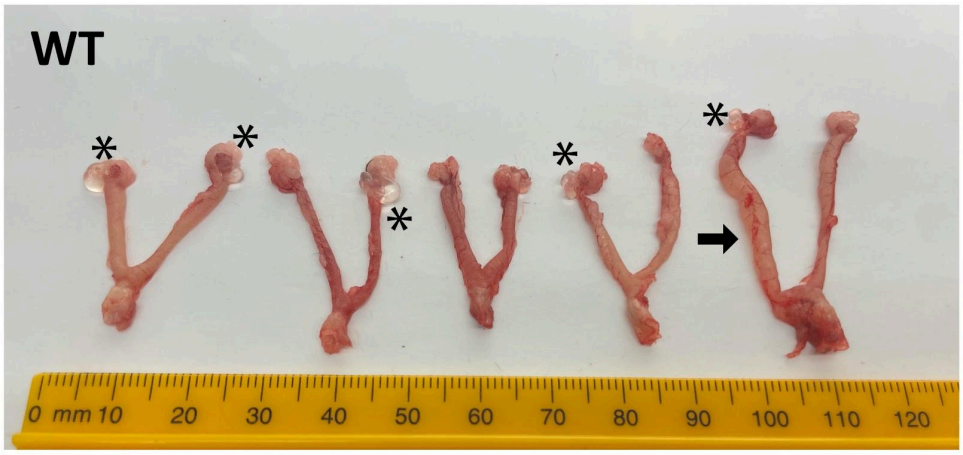
WT
0 mm 10 20 30 40 50 60 70 80 90 100 110 120

B


Δtox
mm 10 20 30 40 50 60 70 80 90 100 110

C

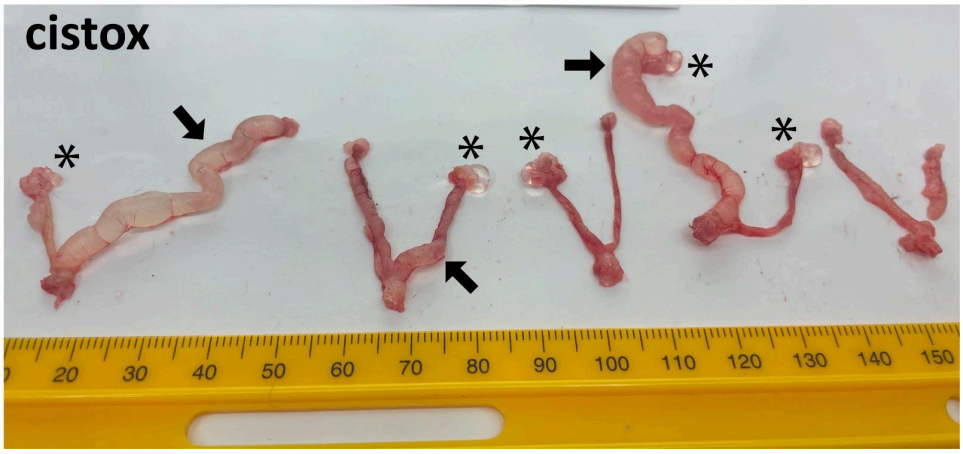
cistox
20 30 40 50 60 70 80 90 100 110 120 130 140 150

Figure 25. Oviduct and uterine gross pathology are reduced during chronic infection with *C. muridarum* Δtox. Gross pathology images of mouse genital tracts transcervically infected with the (A) WT, (B) Δtox, or (C) cistox strains of *C. muridarum* day 51 post transcervical infection. Presence of hydrosalpinx is indicated with a black asterisk, while presence of uterine distension is indicated with a black arrow. Images were taken on via an iPhone 11 camera.

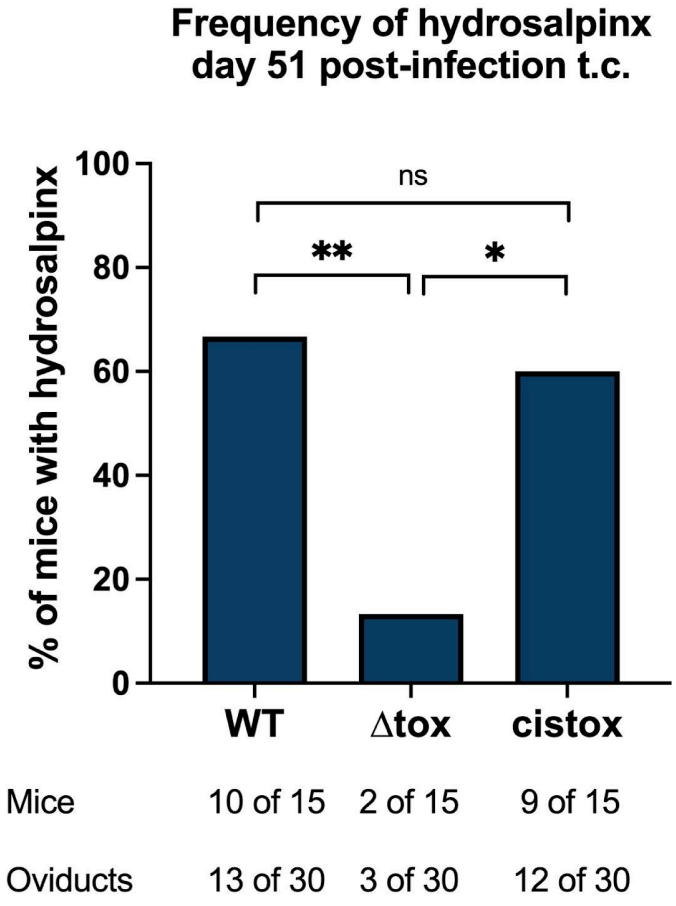

Figure 26. Frequency of hydrosalpinx is significantly reduced during chronic infection with *C. muridarum* Δtox.% of mice with hydrosalpinx was quantified by dividing the number of mice with hydrosalpinx by the total number of mice infected with that strain of the bacteria. Significance was determined by a Fisher's exact test with a p-value of <0.05.

As evident in Figure 25 above, there was a stark difference in gross pathology between the Δtox strain versus the WT and cistox strains. For both the WT and cistox strains, 10 out of 15 mice displayed hydrosalpinx in at least one oviduct, apparent by the presence of clear, glasslike tissue at the end of the uterine horns. Additionally, mice infected with the control strains experienced uterine swelling and distension. This was most prominent in mice infected with cistox, as the uterine horns appeared bulbous, extended, and fluid filled (Figure 25C). In comparison, only 2 of 30 mice infected with Δtox displayed hydrosalpinx, and no mice appeared to have swollen or distended uterine horns (Figure 25B). When the presence of hydrosalpinx was quantified, infection with Δtox resulted in a significant reduction in the percentage of mice with hydrosalpinx in comparison to mice infected with the WT and cistox strains (Figure 26).

2.2.3 Infection with Δtox results in significantly reduced oviduct histopathology during chronic infection

The clear difference in gross pathology between the Δtox and control strains, particularly in regards to hydrosalpinx, prompted us to delve deeper into how these chronic infection phenotypes varied from one another at the cellular level. To do so, the same genital tracts that were assessed for gross pathology on day 51 were sectioned, stained, and analyzed under the microscope so that we could evaluate how these differences appeared during histopathology analysis.

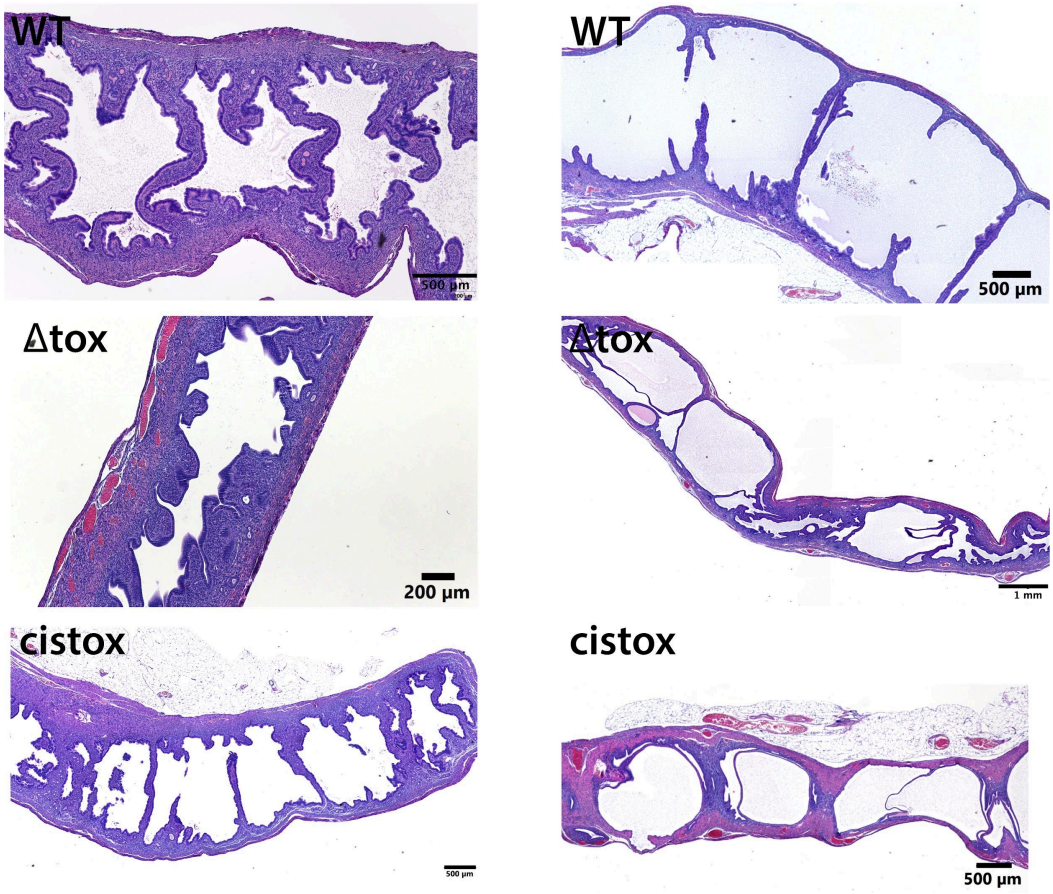

Figure 27. Δtox does not ameliorate uterine horn pathology during chronic upper genital tract infection. H&E stained mouse uteri post transcervical infection with the WT, Δtox, or cistox strains of *C. muridarum*. Different rows indicate tissue infected with different strains. Genital tracts were excised on Day 51 post infection, and sectioned and stained by the Harvard Rodent Histopathology core. Images were photographed via a Pixelink camera on a Nikon Eclipse 50i scope. Images were stitched together via cellSens imaging software and scale bars were added via ImageJ.

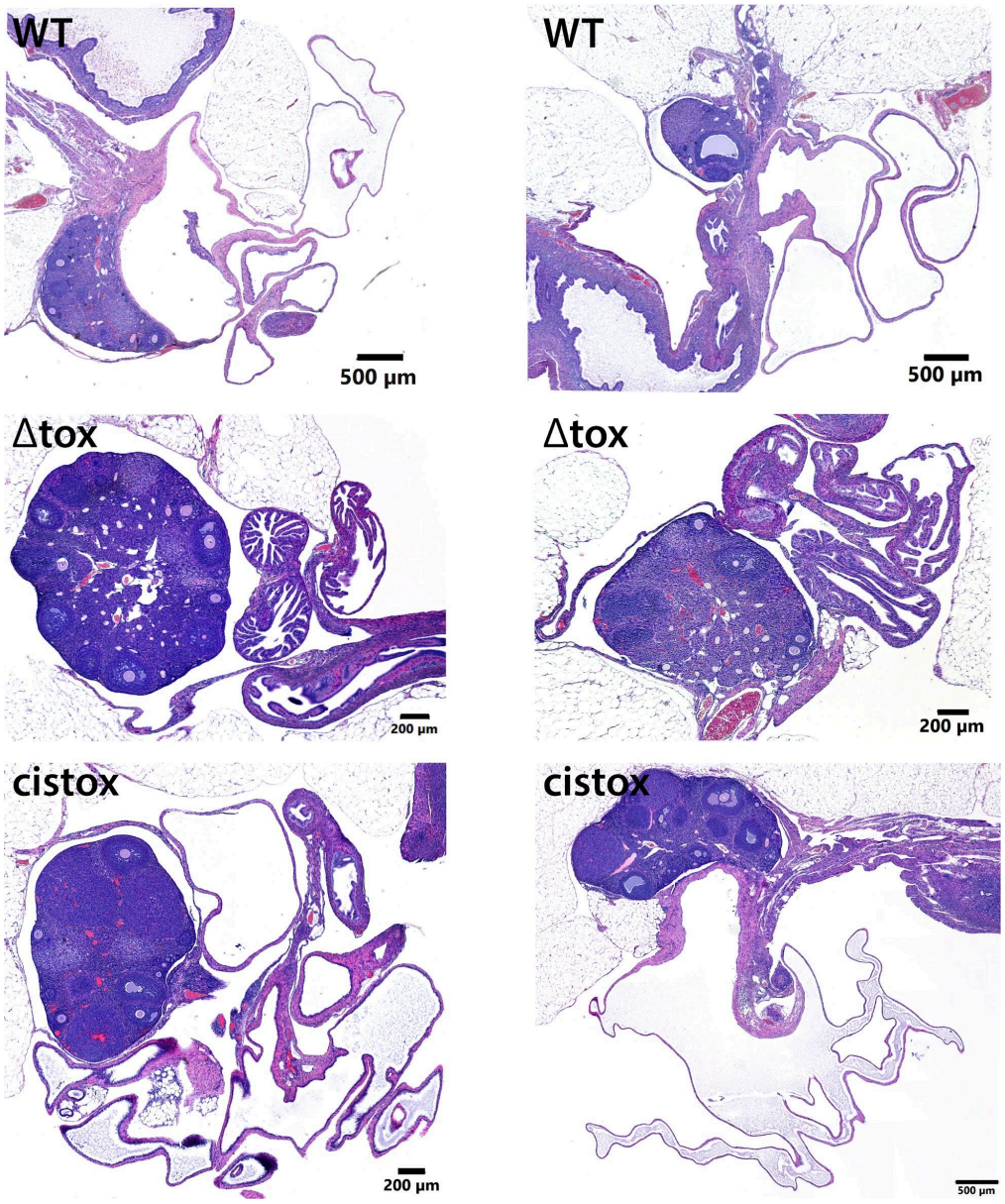

Figure 28. Δtox results in reduced oviduct immunopathology during chronic upper genital tract infection. H&E stained mouse ovaries and oviducts post transcervical infection with the WT, Δtox, or cistox strains of *C. muridarum*. Different rows indicate tissue infected with different strains. Genital tracts were excised on Day 51 post infection, and sectioned and stained by the Harvard Rodent Histopathology core. Images were photographed via a Pixelink camera on a Nikon Eclipse 50i scope. Images were stitched together via cellSens imaging

software and scale bars were added via ImageJ.

Microscopy analysis of the tissue revealed that unlike what we observed at the gross pathology level, uterine horn histopathology was extremely similar across the three strains. Mice infected with Δtox, WT, and cistox all displayed swollen dilated uterine horns that had slight neutrophil infiltration into the lumen (Figure 27). Likewise, the ovaries of mice infected with each of the three strains closely resembled one another, presenting with minimal edema and immune cell infiltration into the ovarian membrane space (Figure 28). However, we did observe a staggering difference in oviduct pathology across the three strains. The oviducts of mice infected with the WT and cistox strains were incredibly swollen, had slight neutrophil infiltration, and appeared as huge empty pockets which no longer contained the invaginations that had previously characterized the tissue (Figure 28). In comparison, oviducts infected with Δtox were clear of immune cells and presented little to no swelling or edema, retaining their characteristic morphology and invaginations.

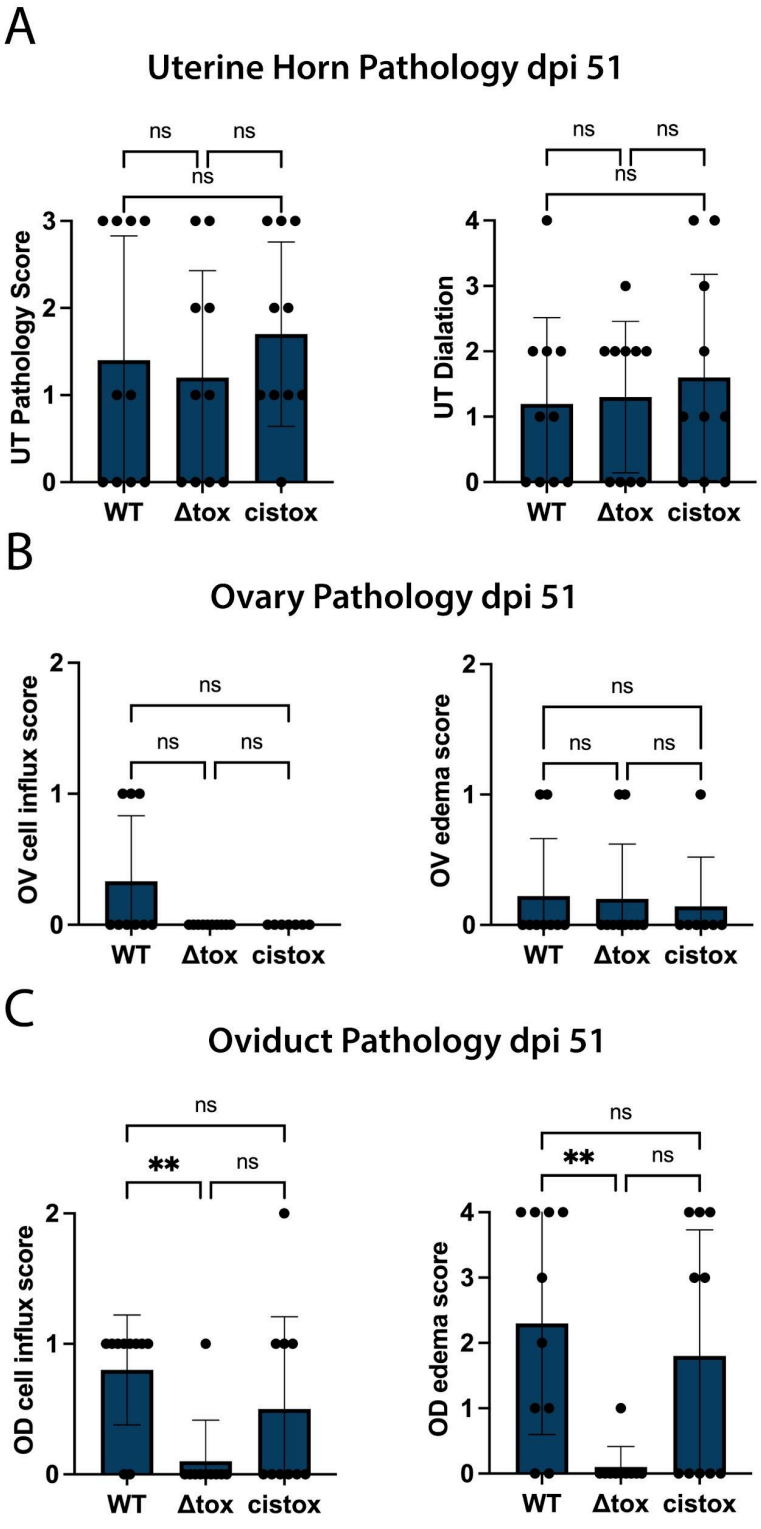
A
Uterine Horn Pathology dpi 51
UT Pathology Score
UT Dialation
ns
WT
Δtox
cistox
B
Ovary Pathology dpi 51
OV cell influx score
OV edema score
C
Oviduct Pathology dpi 51
OD cell influx score
OD edema score
**

Figure 29. Δtox significantly reduces cellular infiltration and edema in the oviducts. Pathology scores were determined in-house via a double-anonymized scoring system. (A) Uterine horns were scored on a scale of 0-3 or 0-4 for general pathology and uterine dilation respectively. (B) Edema and cellular influx in the ovaries was scored using a 0-2 scale. (C) Edema and cellular influx in the oviducts was scored from 0-4 or 0-2 respectively. Higher scores indicated more severe, robust pathology of the tissue. Significance was determined by the Kruskal-Wallis test using a p-value of < 0.01, followed by Dunn's multiple comparisons test.

The anonymized pathology scoring of the tissue closely resembles what we witnessed under the microscope. There were no significant differences in uterine horn pathology or dilation across the three strains (Figure 29A). Similarly, there were also no significant differences in ovarian cellular infiltration or edema upon infection with the Δtox, WT, or cistox strain (Figure 29B). In comparison, there was a significant difference in oviduct pathology between the Δtox and WT strains, as infection with Δtox resulted in reduced cellular infiltration into the oviduct, and reduced oviduct edema (Figure 29C). Coupled to the results of our gross pathology assessment, these findings strongly indicate that during chronic infection, Δtox leads to a reduction in pathology of the oviducts, both at a gross and cellular level.

2.3 Summary of Secondary Results

The key takeaways from the second stage of this investigation are threefold. First, the Δtox strain is capable of infecting the genital tract as effectively as the WT and cistox strains. Second, the Δtox strain is unable to

persist in the lower genital tract as long as the control strains. Third, both acute and chronic infection of the upper genital tract with the Δtox strain of the bacteria result in a significant reduction in oviduct pathology. These findings are incredibly promising and have strong implications for what role the putative virulence factors *tc0437-0439* may play during *Chlamydia* infection.

DISCUSSION

1. Overview of Key Results

Chronic infection with *Chlamydia* is the source of debilitating genital tract disease for millions of people worldwide. Conditions such as pelvic inflammatory disorder and infertility that are caused by the non protective immune response of the host to the bacteria are extremely difficult to treat, and thus preventing them from developing in the first place is of the utmost importance (1,2). However, how exactly *Chlamydia* causes immunopathology and leads to these disease states remains unclear, and thus it is not currently feasible to design an effective vaccine that prevents these conditions from arising.

With this in mind, the central goal of this research has been to better understand how *Chlamydia* causes disease in the upper genital tract. To do so, we investigated a set of open reading frames that 1) were only present in strains of the bacteria that elicited robust immunopathology, and 2) appeared to have cytotoxic capabilities. By infecting mice with a strain of *C. muridarum* in which *tc0437-0439* had been deleted, we were able to identify whether or not these ORFs play a role in inducing immunopathology, and gain a better understanding of the mechanisms they might use to do so. We hypothesized that they serve as virulence factors of the bacteria that drive immunopathology of the upper genital tract and facilitate bacterial invasion of host cells. Thus, removing them from the *C. muridarum* genome would lead to reduced bacterial burden, and reduced

immunopathology of the genital tract. The results from this study can be broken down into two critical findings that address (1) the ability of the Δtox strain to infect the host tissue (2) the ability of Δtox strain to induce pathology of the genital tract.

Chlamydia infection occurs in three stages; the initial infection of the lower genital tract, the ascension of the bacteria to the upper genital tract, and the invasion of the uterine horns, oviducts, and ovaries (9). Throughout our investigation we found that, despite lacking the putative virulence factors, the Δtox strain was able to successfully carry out each of these three stages, as mice infected with the Δtox strain exhibited no difference in early vaginal shedding, ascension, or upper genital tract burden in comparison to mice infected with the control strains. However, our exploration of burden did identify one significant difference between the Δtox and control strains: the ability to persist in the lower genital tract tissue. Unlike the WT and cistox strains which were cleared from the LGT during the late stages of infection, presence of the Δtox strain in the tissue began to diminish as early as 11 days post infection, and the bacteria was completely cleared from the LGT 7 days earlier than the control strains. Taken together this burden data indicates that the absence of *tc0437-0439* from the *C. muridarum* genome does not impact the ability of the bacteria to establish infection in vivo, however it does reduce the capacity of the bacteria to persist in the lower genital tract at later time points of infection.

By conducting an in depth analysis of histopathology, we next identified that infection with the Δtox strain resulted in significantly reduced immunopathology of the oviducts. While a decrease in pathology was already evident during the acute, early stages of infection, this reduction was particularly pronounced during chronic infection, as we saw a decrease in oviduct pathology at both the cellular level and the macroscopic level. At the cellular level this manifested as a reduction in immune cell infiltration into the oviduct lumen, and a lack of swelling or edema of the tissue. At the macroscopic level this was evident as a significant amelioration of hydrosalpinx in mice infected with the Δtox strain compared to mice infected with the control strains. These findings suggest two critical concepts: these putative cytotoxin ORFs are necessary to induce immunopathology of the oviducts during genital tract infection, and these ORFs play a role in the development of hydrosalpinx during chronic *Chlamydia* infection.

Individually, these results offer different insights into how these putative virulence factors impact *Chlamydia* infection in vivo. However, to gain a more comprehensive understanding of their function and potential mechanisms of action, it is critical to interpret these findings together. Our burden data demonstrates that the Δtox strain is able to successfully invade the genital tract, meaning that infection with any of the three strains, mutant or control, results in the same amount of bacteria present in the upper genital tract tissue. In spite of this, we see a difference in how much oviduct pathology develops upon infection

with the Δtox strain compared to the controls. This suggests that the decrease in oviduct pathology that occurs during Δtox infection is not the result of the ability of the bacteria to invade and infect host cells of the upper genital tract. However, our burden data also indicates that the Δtox strain is cleared from the lower genital tract much earlier than the control strains, suggesting that *tc0437-0439* may also play a role in the ability of the bacteria to persist in the lower genital tract. Altogether this implies that these putative virulence factors contribute to oviduct pathology during *Chlamydia* infection, and that they may do so in two different ways, depending on the tissue with which they are interacting. In the lower gential tract, these ORFs may facilitate bacterial persistence, while in the upper genital tract they may contribute to oviduct pathology via a burden independent mechanism.

2. Potential Mechanisms of Action

Our findings strongly suggest that these putative virulence factors play a critical role in eliciting oviduct immunopathology and hydrosalpinx during *Chlamydia* infection. The results of our burden experiments demonstrate that these ORFs appear to contribute to this pathology in two different ways, depending on which tissue of the genital tract the bacteria is interacting with. However, as these are novel results and the ORFs had yet to be linked to disease in the oviducts, the exact mechanism with which they accomplish this remains unclear.

2.1 Burden Independent Mechanism

When in the upper genital tract, the function of these ORFs can be decoupled from the ability of the bacteria to invade host cells. This suggests that the influence they exert on oviduct pathology occurs after *Chlamydia* has established infection in the UGT. Thus, to better understand how these putative virulence factors function to elicit oviduct disease during upper genital tract infection, we must also consider the host factors involved.

Chen et al. conducted a study which investigated the development of hydrosalpinx in 11 distinct strains of mice. They found that different strains displayed varying levels of susceptibility to hydrosalpinx upon infection with *C. muridarum*. More specifically, some strains of mice were highly susceptible, some were moderately susceptible, and a few appeared to be completely resistant, developing no hydrosalpinx whatsoever. To determine what the reason for this variation might be, they measured the expression of pro-inflammatory cytokines, signaling molecules that promote inflammation, in the ovarian/oviduct tissue of the different types of mice. Notably, they found that mice that were highly susceptible to hydrosalpinx displayed increased expression of 27 pro-inflammatory cytokines relative to the resistant strains. One of these cytokines, known as IL-1α, was dramatically increased in mice that readily developed robust oviduct pathology (32). This was echoed by Yang et al. in their study of hydrosalpinx, as they identified a 5.5 fold increase in IL-1α expression in mice who developed hydrosalpinx compared to mice who did not (37).

A pro-inflammatory cytokine that is constitutively expressed in epithelial cells, IL-1α production is upregulated upon exposure to various stimuli such as foreign material or pathogens. However, IL-1α also functions as an alarmin, a signaling molecule that is released from damaged or dying cells as a means of triggering an inflammatory response (38, 39). Upon activation, IL-1α promotes neutrophil recruitment to the site of infection or damage, and activates fibroblasts, a group of cells which facilitate fibrosis and scarring. Dysregulation of IL-1α is highly associated with auto-immune disorders, as the release of the cytokine in response to cell death further promotes tissue damage, perpetuating a cycle of persistent inflammation (38). Gyorke et al. recently published a paper exploring the role of IL-1α in the development of oviduct pathology during *C. muridarum* infection in mice. To perform this study, they infected mice that were deficient in IL-1α (*Il1a*$^{-/-}$ mice) with *C. muridarum*, and assessed gross pathology, histopathology, and burden (39).

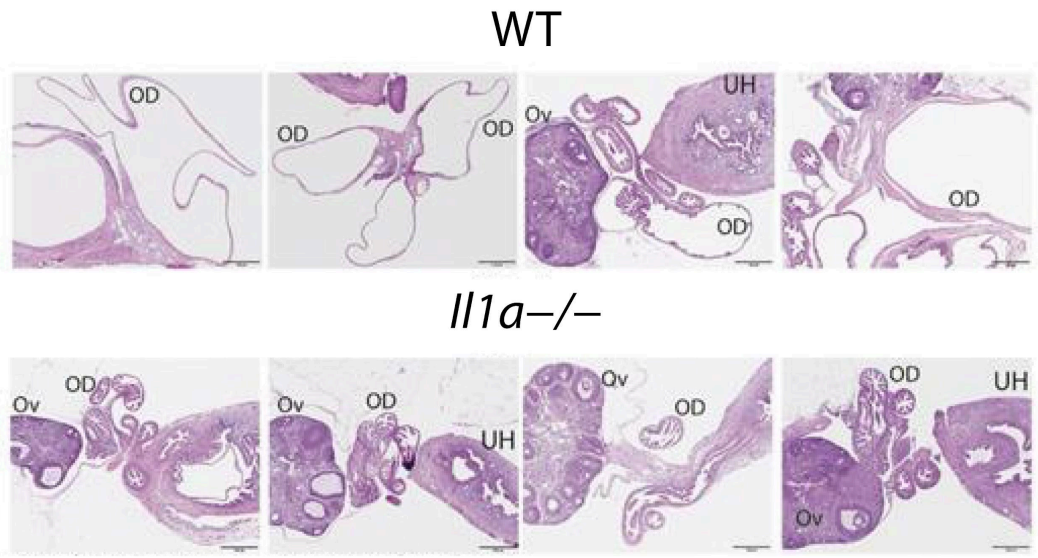

Figure 30. Mice deficient in IL-1α exhibit reduced oviduct pathology. in WT (top) and *Il1a*$^{-/-}$ (bottom) mice on day 45 post transcervical *C. muridarum* infection. OD = Oviduct, Ov = Ovary, and UH = Uterine Horn. Figure was adapted from Gyorke et al.

Their results indicated that, despite exhibiting similar levels of UGT burden, mice deficient in IL-1α displayed a significant reduction in hydrosalpinx and oviduct histopathology compared to the WT mice. Pathology in *Il1a*$^{-/-}$ mice was marked by a reduction in oviduct dilation and the retention of oviduct invaginations relative to the WT mice (Figure 30). Strikingly, these results were extremely similar to those of our own histopathology analysis, with this reduction in oviduct immunopathology in *Il1a*$^{-/-}$ mice modelling that which occurs upon infection with the Δtox strain of *C. muridarum* (39).

On top of their pathology and burden data, Gyorke et al. noted an additional critical finding: In WT mice, IL-1α expression persisted in the tissue

even after the bacteria had been cleared. Thus their study demonstrates that IL-1α is essential for oviduct pathology and hydrosalpinx during *Chlamydia* infection and suggests that persistent production of the cytokine after clearance may contribute to the severe damage we see during chronic infection (39).

As previously discussed, our putative virulence factors share strong sequence similarity with *C. difficile* cytotoxins TcdA and TcdB. Both of these *C. difficile* proteins function as glycosyltransferases that disrupt the actin cytoskeletons of host cells, causing cell damage and killing cells. Cell culture studies performed by Thalmann et al. suggest that our *Chlamydia* ORFs encode proteins that contain a similar cytotoxic nature, as they display the ability to remodel the actin cytoskeleton, causing cell rounding and cell death (27). As IL-1α functions as an alarmin that is expressed by damaged and dying cells, it is possible that one mechanism with which these *Chlamydia* ORFs induce oviduct pathology is by upregulating IL-1α expression through cytotoxic activity. By damaging and killing cells of the upper genital tract, the putative cytotoxins would trigger the robust expression of the pro-inflammatory cytokine. The persistence of IL-1α in the tissue even upon bacterial clearance would result in the development of severe oviduct pathology, and hydrosalpinx.

Although this mechanism of action appears promising, having yet to explore the interactions of our putative toxin genes with the host factors responsible for oviduct pathology, we cannot say with certainty that this is the pathway that these ORFs utilize to cause oviduct disease. Multiple other features

of the immune system have been implicated in the development of hydrosalpinx, including the complement system - a critical element of the innate immune response - and caspase 11 - a proteolytic enzyme involved in apoptosis - as deficiencies in both of these components of the immune system results in reduced oviduct pathology (37), (40). Thus, to identify the exact mechanisms at play here, further studies into the interactions of these virulence factors with the host immune response in the upper genital tract are imperative.

2.2 Persistence mechanism

While there is strong evidence that these virulence factors act as cytotoxins that drive oviduct pathology during upper genital tract infection, there is emerging research which suggests that these ORFS may also contribute to oviduct disease via another function when the bacteria is in the lower genital tract. Our assessment of vaginal shedding identified that these ORFs influence the ability of the bacteria to maintain infection and persist within the lower genital tract tissue. *Chlamydia* persistence has been implicated in the development of disease sequelae, as the prolonged presence of the bacteria within the host contributes to continuous inflammation that results in severe tissue damage. This suggests that these virulence factors may elicit oviduct pathology by facilitating bacterial survival within the lower genital tract. This conjecture is supported by the recent findings of our collaborators in the Fields lab. Via cell culture studies, they identified that the proteins encoded by these ORFs are not secreted, like most

cytotoxins are, but instead are surface localized . Surface localized proteins sit at the interface between host cells and the bacteria, and often play a role in cell attachment and invasion. The ability of the bacteria to invade and infect host cells is critical for *Chlamydia* to be able to persist within the host tissue, as it ensures that the bacteria has access to nutrients and can evade the protective immune response (41). Thus, the findings of the Fields lab coupled to our vaginal shedding results suggest that in the lower genital tract, these ORFS may function by facilitating host cell invasion, allowing for bacterial persistence within the tissue and the subsequent development of disease sequelae such as hydrosalpinx.

It is important to reiterate that this function appears to be tissue specific. We recently performed an experiment assessing UGT burden at late time points after transcervical infection. We found that all three strains of the bacteria – Δtox, WT, and cistox – were completely cleared from the UGT, suggesting that these ORFs do not contribute to the ability of the bacteria to persist in the upper genital tract like they do in the lower genital tract. This data was not shown in this study, as we have yet to run the necessary controls to precisely define what our limit of detection of *Chlamydia* 16S DNA is (Appendix C.3). Thus this novel non-cytotoxic function of these ORFs appears to be tissue-specific, and only occurs upon interaction with cells of the lower genital tract.

Chlamydia is widely considered to be a tissue tropic disease. Different serovars of the bacteria preferentially infect different locations in the body: Serovars A-C infect the eyes, serovars D-K infect the genital tract, and serovars

L1-L3 establish infection in the lymph nodes (3,4). The key to this variability in tropism is genetic diversity, as the expression of different proteins is strongly associated with where the bacteria infects, and how robust of an infection it elicits. The reason for this being that virulence factors of the bacteria respond differently to distinct tissue and cell types (42). Thus, our conjecture that these ORFs take on a different function depending on which tissue of the genital tract they encounter aligns with the behavior of other *Chlamydia* proteins. However, it remains unclear how exactly interactions with different tissue types mediate a change in the function of these virulence factors. *Chlamydia* establishes infection through the invasion of epithelial cells (9). The epithelial cell of the endocervix (the site of infection in the lower genital tract), and the oviduct (the primary site of pathology in the upper genital tract) differ from one another in terms of morphology and function (43, 44). However, how they vary in regards to which cell surface receptors they express, in particular those involved in *Chlamydia* invasion, remains unclear and not well studied. Thus, to better understand how the proteins encoded by these ORFs may facilitate invasion in one cell type but not another, it is necessary to more closely analyze and compare the cell surface proteins of these two epithelial cell types.

Despite these unknowns, the possibility that these putative virulence factors may take on different functions in the lower genital tract compared to the upper genital tract to induce oviduct pathology is incredibly exciting. It highlights the central finding of this research, which is that these ORFs act as virulence

factors during *Chlamydia* infection, and it offers up different avenues for future vaccines which may target the proteins encoded by these ORFs.

3. Obstacles throughout the study

Throughout this investigation, there were three central obstacles that we needed to contend with or adapt around in order to effectively answer our research question: 1) The need to use a murine species of the bacteria to study a human pathogen, 2) The use of a mouse model to study a human disease, and 3) The absence of the complemented strain for a better part of the experiment.

3.1 Usage of a murine pathogen

To best understand how *Chlamydia* causes long lasting sequelae in humans, it is of course ideal to work with the species of the bacteria that naturally infects humans, *C. trachomatis*. However for this specific investigation, this was neither feasible nor ideal. As *C. trachomatis* is not readily genetically mutated, generating a mutant strain of the bacteria in which CT166 was deleted from the genome proved incredibly difficult. The Fields lab at the University of Kentucky Medical School with whom we collaborated on this research are the leading experts in *Chlamydia* genetics. However, they were unable to remove CT166 from the *C. trachomatis* genome. They were however, able to remove tc0437-0439 from the *C. muridarum* genome, producing viable *Chlamydia* EBS that were lacking these ORFs. Thus, working with *C. muridarum* offered a

promising alternative in order to study how the deletion of these ORFs impacts the ability of *Chlamydia* to cause disease.

In addition, *C. muridarum* is the ideal species of the bacteria to study when using a mouse model to investigate how *Chlamydia* causes disease. Not only is *C. trachomatis* not capable of eliciting the same robust pathology and disease in mice that it does in humans, but the bacteria must be administered transcervically, which limits our ability to study ascension and lower genital tract burden (45). In comparison, *C. muridarum* infection of the murine genital tract closely resembles *C. trachomatis* infection in humans in terms of both severity and duration, and the bacteria can be administered intravaginally or transcervically, addressing this limitation of the human pathogen (13).

3.2 Usage of a mouse model

The central goal of this research is to gain an understanding of how *Chlamydia* causes disease in humans. Thus, it would be most informative for us to study how pathology develops in humans directly. However, this is extremely challenging for three main reasons: 1) The human population is highly variable. Different individuals have different genetic makeups, possess unique health histories, and make different lifestyle choices. This variability makes it incredibly difficult to collect data that is not influenced by external factors, and thus results obtained from human samples are oftentimes not applicable for the global population. 2) *Chlamydia* infection is localized to the upper genital tract. It is

extremely difficult to collect sample tissue of the ovaries, oviducts, or uterus, especially to monitor how infection characteristics change or develop over time. 3) Most importantly, to effectively study how *Chlamydia* disease progresses from the initiation of infection to the development of sequelae, it would be necessary to actively infect humans with the bacteria and allow for disease to develop, which is unethical.

For these reasons, it was imperative to conduct this research using a model organism. Mouse models are the ideal animal model to study *Chlamydia*, as they are extremely similar to humans in terms of both genetics and genital tract anatomy, they allow for greater control over experimental variables, and they are the most commonly used model in the *Chlamydia* field (45,46). Thus, any results we obtained would uphold the experimental standard of the field and allow us to constructively compare our results to pre-existing studies. However, because this study was performed in mice, it is critical that when interpreting our results we recognize that they may not be directly translatable to humans. Our results instead should be regarded as the necessary first steps to be able to address the larger overarching question of how to prevent *Chlamydia* disease in humans.

3.3 Absence of the cistox strain throughout the preliminary stage

The complemented cistox strain serves as a critical control in our investigation, as it allows us to determine whether any differences that arise upon infection with the Δtox strain can be attributed to the function of our putative

virulence factors, or whether they occur because of the genetic manipulation of the bacteria's genome. Unfortunately, the complemented strain had not been generated when we began this study, and thus we were unable to include it in the preliminary experiments we conducted. However, while these preliminary studies offered valuable data and results, its primary goals were to identify if a genetic approach in vivo was an effective means of answering our research question, and whether or not our methodologies allowed for us to collect valuable data. The absence of the complemented strain from these experiments did not hinder our ability to address these questions, and thus did not take away from their results. Additionally, the secondary stage of this study was either similar to or an exact repeat of each experiment performed in the preliminary stage, and thus we were able to observe how infection with the Δtox and WT strains compared to infection with the cistox strain for each aspect of burden and pathology that we were investigating.

4. Future directions

The promising nature of the results from this research strongly indicate that further investigation into these virulence factors is both warranted and necessary. Thus, there are multiple next steps that we intend to take in order to delve further into the role of these ORFs in eliciting oviduct pathology and causing disease during *Chlamydia* infection.

First, by continuing to collaborate with the Fields lab, we intend to repeat these experiments with different variations of the Δtox strain. The Δtox strain was generated by deleting all three open reading frames - tc0437, tc0438, and tc0439 - from the *C. muridarum* genome. However, the role of each of these individual open reading frames remains unclear. How they contribute to pathology individually can be unpacked by generating new single deletion strains of *C. muridarum* in which only one of the ORFs has been removed from the genome. By infecting mice with these different mutant strains and assessing how pathology changes, we can begin to discern their individual contributions to the Δtox phenotype that we observed in this study, and identify if all three ORFs are necessary to cause oviduct disease, or if one of them plays a more pivotal role.

Additionally, we intend to repeat this study using the *C. trachomatis* serovar D mutant in which CT166 has been deleted from the genome. While the Fields lab has yet to generate this mutant strain, they continue to make progress towards creating viable EBs of the bacteria that are lacking this ORF. As discussed earlier, *C. trachomatis* serovar D does not elicit robust pathology in mice to the same extent that it does in human, and thus *C. muridarum* was our preferred strain to study in order to clearly identify how these putative virulence factors impacted the ability of the bacteria to cause disease. However, knowing now how these ORFs contribute to *Chlamydia* infection, it is of great value to repeat this experiment with the human pathogen and determine whether or not there is an amelioration of oviduct pathology similar to that which we observe

with the Δtox strain. If the results from this next step are consistent with what we identified in this study, this will give us further insight into how to treat and prevent *Chlamydia* infection in humans.

Furthermore, having used a genetic approach to identify that tc0437-0439 drive oviduct pathology during *C. muridarum* infection, it is our intention to next use an immunological approach to further assess how these ORFs contribute to *Chlamydia* disease. To do so, we plan to perform a vaccine study that closely resembles our pilot experiment assessing the impact of immunization against CT166 on immunopathology of the upper genital tract. In this pilot study, we designed a vaccine in which CT166 peptides were chemically conjugated to a virus-like particle vector known as Qβ. Mice were immunized with the vaccine, challenged with *C. trachomatis*, and histopathology was then assessed. Our future vaccine study would replicate this methodology, but instead conjugate tc0437, tc0438, and tc0439 peptides to Qβ, and challenge mice with *C. muridarum*. The goal of our pilot study was to gain a sense of whether or not CT166 had the potential to act as a virulence factor in vivo. Coupled to our findings from this study, taking an immunological approach this time would serve a greater purpose, as performing this experiment would allow us to determine whether or not these virulence factors serve as promising targets for a vaccine that aims to reduce oviduct disease during *Chlamydia* infection.

5. Conclusions

The results we obtained throughout this investigation are incredibly promising as they have strong implications for *Chlamydia* research and our capacity to address how this bacteria causes disease. By taking a genetic approach in vivo, we identified that these open reading frames act as virulence factors that drive robust oviduct pathology during *Chlamydia* infection. We also identified that these ORFs may take on different functions to elicit this pathology depending on which genital tract tissue they encounter: In the lower genital tract, these virulence factors appear to facilitate bacterial persistence by promoting host cell invasion, and in the upper genital tract they appear to act as cytotoxins that elicit immunopathology in a burden-independent way. Although these ORFs had previously been identified as potential virulence factors of the bacteria, these findings are novel, as their function in vivo had yet to be investigated until this study. Thus, as this research discerned a critical feature of *Chlamydia* pathogenesis and disease development, it has addressed a prevalent knowledge gap that existed in *Chlamydia* research.

Chlamydia is a ruthless bacteria. The asymptomatic chronic nature of its infection results in the development of painful and debilitating disease which impacts countless people worldwide. At the forefront of this disease state is fallopian tube – or oviduct – pathology, as the ability of the bacteria to induce persistent inflammation and immunopathology in this tissue leads to the development of conditions such as hydrosalpinx. The severe swelling and build

up of fluid that characterizes hydrosalpinx causes extensive damage to the reproductive tract, and thus often results in ectopic pregnancy and infertility. While you can treat an acute *Chlamydia* infection with doxycycline or azithromycin, there is no standard treatment for these chronic disease sequelae, meaning that it is imperative that we develop a vaccine that prevents them from arising in the first place. Demonstrating that these open reading frames serve as virulence factors of *Chlamydia* that drive oviduct disease is groundbreaking and incredibly valuable, as it means we have identified a potential target for a vaccine that specifically addresses the development of oviduct pathology, and therefore disease sequelae, during upper genital tract infection. Thus, this research is the critical first step to developing a targeted, effective *Chlamydia* vaccine that hopes to prevent the suffering of millions around the globe.

LITERATURE CITED

1. *Sexually transmitted infections (STIs)*. (n.d.). Retrieved February 12, 2025, from https://www.who.int/news-room/fact-sheets/detail/sexually-transmitted-infections-(stis)
2. Grygiel-Górniak, B., & Folga, B. A. (2023). Chlamydia trachomatis—An Emerging Old Entity? *Microorganisms*, *11*(5), Article 5. https://doi.org/10.3390/microorganisms11051283
3. Murray, S. M., & McKay, P. F. (2021). Chlamydia trachomatis: Cell biology, immunology and vaccination. *Vaccine*, *39*(22), 2965–2975. https://doi.org/10.1016/j.vaccine.2021.03.043
4. Witkin, S. S., Minis, E., Athanasiou, A., Leizer, J., & Linhares, I. M. (2017). Chlamydia trachomatis: The Persistent Pathogen. *Clinical and Vaccine Immunology : CVI*, *24*(10), e00203-17. https://doi.org/10.1128/CVI.00203-17
5. Lijek, R. S., Helble, J. D., Olive, A. J., Seiger, K. W., & Starnbach, M. N. (2018). Pathology after Chlamydia trachomatis infection is driven by nonprotective immune cells that are distinct from protective populations. *Proceedings of the National Academy of Sciences of the United States of America*, *115*(9), 2216–2221. https://doi.org/10.1073/pnas.1711356115
6. Murthy, A. K., Li, W., & Ramsey, K. H. (2018). Immunopathogenesis of Chlamydial Infections. *Current Topics in Microbiology and Immunology*, *412*, 183–215. https://doi.org/10.1007/82_2016_18
7. Belland, R. J., Scidmore, M. A., Crane, D. D., Hogan, D. M., Whitmire, W., McClarty, G., & Caldwell, H. D. (2001). Chlamydia trachomatis cytotoxicity associated with complete and partial cytotoxin genes. *Proceedings of the National Academy of Sciences*, *98*(24), 13984–13989. https://doi.org/10.1073/pnas.241377698
8. *Chlamydia (Chlamydial Genitourinary Infections): Background, Pathophysiology, Etiology*. (2025). https://emedicine.medscape.com/article/214823-overview?form=fpf
9. Agrawal, T., Vats, V., Salhan, S., & Mittal, A. (2009). The mucosal immune response to *Chlamydia trachomatis* infection of the reproductive tract in women. *Journal of Reproductive Immunology*, *83*(1), 173–178. https://doi.org/10.1016/j.jri.2009.07.013
10. Caven, L. T., & Carabeo, R. A. (2023). The role of infected epithelial cells in Chlamydia-associated fibrosis. *Frontiers in Cellular and Infection Microbiology*, *13*, 1208302. https://doi.org/10.3389/fcimb.2023.1208302
11. El-Kharoubi A. F. (2023). Tubal Pathologies and Fertility Outcomes: A Review. *Cureus*, *15*(5), e38881. https://doi.org/10.7759/cureus.38881
12. De Clercq, E., Kalmar, I., & Vanrompay, D. (2013). Animal Models for Studying Female Genital Tract Infection with Chlamydia trachomatis.

Infection and Immunity, *81*(9), 3060–3067. https://doi.org/10.1128/IAI.00357-13
13. Wang, Y., Han, Z., Wang, L., Sun, X., Tian, Q., & Zhang, T. (2025). Development and Validation of Chlamydia muridarum Mouse Models for Studying Genital Tract Infection Pathogenesis. *Bio-Protocol*, *15*(3), e5181. https://doi.org/10.21769/BioProtoc.5181
14. Owen, J. A., Punt, J., Stranford, S. A., Jones, P. P., & Kuby, J. (2013). *Kuby immunology* (Seventh edition.). W.H. Freeman.
15. Marshall, J. S., Warrington, R., Watson, W., & Kim, H. L. (2018). An introduction to immunology and immunopathology. *Allergy, asthma, and clinical immunology : official journal of the Canadian Society of Allergy and Clinical Immunology*, *14*(Suppl 2), 49. https://doi.org/10.1186/s13223-018-0278-1
16. Brunham, R. C., & Rey-Ladino, J. (2005). Immunology of Chlamydia infection: implications for a Chlamydia trachomatis vaccine. *Nature reviews. Immunology*, *5*(2), 149–161. https://doi.org/10.1038/nri1551
17. Wang, X., Wu, H., Fang, C., & Li, Z. (2024). Insights into innate immune cell evasion by Chlamydia trachomatis. *Frontiers in Immunology*, *15*, 1289644. https://doi.org/10.3389/fimmu.2024.1289644
18. Wilton, Z. E. R., Jamus, A. N., Core, S. B., & Frietze, K. M. (2025). Pathogenic and Protective Roles of Neutrophils in Chlamydia trachomatis Infection. *Pathogens*, *14*(2), 112. https://doi.org/10.3390/pathogens14020112
19. McGavern, D. B. (2005). The Role of Bystander T Cells in CNS Pathology and Pathogen Clearance. *Critical Reviews in Immunology*, *25*(4), 289–303.
20. Abdelrahman, Y. M., & Belland, R. J. (2005). The chlamydial developmental cycle. *FEMS microbiology reviews*, *29*(5), 949–959. https://doi.org/10.1016/j.femsre.2005.03.002
21. Kellogg, K. R., Horoschak, K. D., & Moulder, J. W. (1977). Toxicity of Low and Moderate Multiplicities of Chlamydia psittaci for Mouse Fibroblasts (L Cells). *Infection and Immunity*, *18*(2), 531–541.
22. Read, T. D., Brunham, R. C., Shen, C., Gill, S. R., Heidelberg, J. F., White, O., Hickey, E. K., Peterson, J., Utterback, T., Berry, K., Bass, S., Linher, K., Weidman, J., Khouri, H., Craven, B., Bowman, C., Dodson, R., Gwinn, M., Nelson, W., … Fraser, C. M. (2000). Genome sequences of Chlamydia trachomatis MoPn and Chlamydia pneumoniae AR39. *Nucleic Acids Research*, *28*(6), 1397–1406.
23. Shen, A. (2012). Clostridium difficile Toxins: Mediators of Inflammation. *Journal of Innate Immunity*, *4*(2), 149–158. https://doi.org/10.1159/000332946
24. Carter, G. P., Chakravorty, A., Pham Nguyen, T. A., Mileto, S., Schreiber, F., Li, L., Howarth, P., Clare, S., Cunningham, B., Sambol, S. P., Cheknis, A., Figueroa, I., Johnson, S., Gerding, D., Rood, J. I., Dougan, G., Lawley,

T. D., & Lyras, D. (2015). Defining the Roles of TcdA and TcdB in Localized Gastrointestinal Disease, Systemic Organ Damage, and the Host Response during Clostridium difficile Infections. *mBio*, *6*(3), e00551-15. https://doi.org/10.1128/mBio.00551-15

25. Bothe, M., Dutow, P., Pich, A., Genth, H., & Klos, A. (2015). DXD Motif-Dependent and -Independent Effects of the *Chlamydia trachomatis* Cytotoxin CT166. *Toxins*, *7*(2), 621-637. https://doi.org/10.3390/toxins7020621
26. Chin, E., Kirker, K., Zuck, M., James, G., & Hybiske, K. (2012). Actin recruitment to the Chlamydia inclusion is spatiotemporally regulated by a mechanism that requires host and bacterial factors. *PloS one*, *7*(10), e46949. https://doi.org/10.1371/journal.pone.0046949
27. Thalmann, J., Janik, K., May, M., Sommer, K., Ebeling, J., Hofmann, F., Genth, H., & Klos, A. (2010). Actin Re-Organization Induced by Chlamydia trachomatis Serovar D - Evidence for a Critical Role of the Effector Protein CT166 Targeting Rac. *PLoS ONE*, *5*(3), e9887. https://doi.org/10.1371/journal.pone.0009887
28. Gondek, D. C., Olive, A. J., Stary, G., & Starnbach, M. N. (2012). CD4+ T cells are necessary and sufficient to confer protection against C. trachomatis infection in the murine upper genital tract. *Journal of Immunology (Baltimore, Md. : 1950)*, *189*(5), 2441–2449. https://doi.org/10.4049/jimmunol.1103032
29. Morrison, S. G., Farris, C. M., Sturdevant, G. L., Whitmire, W. M., & Morrison, R. P. (2011). Murine Chlamydia trachomatis Genital Infection Is Unaltered by Depletion of CD4+ T cells and Diminished Adaptive Immunity. *The Journal of Infectious Diseases*, *203*(8), 1120–1128. https://doi.org/10.1093/infdis/jiq176
30. Rixon, J. A., Fong, K. D., Morris, C., Nguyen, A. T., Depew, C. E., & McSorley, S. J. (2024). Elimination of Chlamydia muridarum from the female reproductive tract is IL-12p40 dependent, but independent of Th1 and Th2 cells. *PLOS Pathogens*, *20*(1), e1011914. https://doi.org/10.1371/journal.ppat.1011914
31. Darville, T., Andrews, C. W., Laffoon, K. K., Shymasani, W., Kishen, L. R., & Rank, R. G. (1997). Mouse strain-dependent variation in the course and outcome of chlamydial genital tract infection is associated with differences in host response. *Infection and Immunity*, *65*(8), 3065–3073.
32. Chen, J., Zhang, H., Zhou, Z., Yang, Z., Ding, Y., Zhou, Z., Zhong, E., Arulanandam, B., Baseman, J., & Zhong, G. (2014). Chlamydial Induction of Hydrosalpinx in 11 Strains of Mice Reveals Multiple Host Mechanisms for Preventing Upper Genital Tract Pathology. *PLOS ONE*, *9*(4), e95076. https://doi.org/10.1371/journal.pone.0095076
33. Dockterman, J., & Coers, J. (2021). Immunopathogenesis of genital Chlamydia infection: Insights from mouse models. *Pathogens and Disease*, *79*(4), ftab012. https://doi.org/10.1093/femspd/ftab012

34. Zhang, H., Zhou, Z., Chen, J., Wu, G., Yang, Z., Zhou, Z., Baseman, J., Zhang, J., Reddick, R. L., & Zhong, G. (2014). Lack of Long-Lasting Hydrosalpinx in A/J Mice Correlates with Rapid but Transient Chlamydial Ascension and Neutrophil Recruitment in the Oviduct following Intravaginal Inoculation with Chlamydia muridarum. *Infection and Immunity*, *82*(7), 2688–2696. https://doi.org/10.1128/iai.00055-14
35. Callan, T., Woodcock, S., & Huston, W. M. (2021). Ascension of Chlamydia is moderated by uterine peristalsis and the neutrophil response to infection. *PLoS Computational Biology*, *17*(9), e1009365. https://doi.org/10.1371/journal.pcbi.1009365
36. Mpiga, P., & Ravaoarinoro, M. (2006). Chlamydia trachomatis persistence: An update. *Microbiological Research*, *161*(1), 9–19. https://doi.org/10.1016/j.micres.2005.04.004
37. Yang, Z., Conrad, T., Zhou, Z., Chen, J., Dutow, P., Klos, A., & Zhong, G. (2014). Complement Factor C5 but Not C3 Contributes Significantly to Hydrosalpinx Development in Mice Infected with Chlamydia muridarum. *Infection and Immunity*, *82*(8), 3154–3163. https://doi.org/10.1128/IAI.01833-14
38. Malik, A., & Kanneganti, T.-D. (2018). Function and regulation of IL-1α in inflammatory diseases and cancer. *Immunological Reviews*, *281*(1), 124–137. https://doi.org/10.1111/imr.12615
39. Gyorke, C. E., Kollipara, A., Allen, J., IV, Zhang, Y., Ezzell, J. A., Darville, T., Montgomery, S. A., & Nagarajan, U. M. (2020). IL-1α Is Essential for Oviduct Pathology during Genital Chlamydial Infection in Mice. *The Journal of Immunology*, *205*(11), 3037–3049. https://doi.org/10.4049/jimmunol.2000600
40. Allen, J., Gyorke, C. E., Tripathy, M. K., Zhang, Y., Lovett, A., Montgomery, S. A., & Nagarajan, U. M. (2019). Caspase-11 Contributes to Oviduct Pathology during Genital Chlamydia Infection in Mice. *Infection and Immunity*, *87*(8), e00262-19. https://doi.org/10.1128/IAI.00262-19
41. Gitsels, A., Sanders, N., & Vanrompay, D. (2019). Chlamydial Infection From Outside to Inside. *Frontiers in Microbiology*, *10*. https://doi.org/10.3389/fmicb.2019.02329
42. Abdelsamed, H., Peters, J., & Byrne, G. I. (2013). Genetic variation in Chlamydia trachomatis and their hosts: Impact on disease severity and tissue tropism. *Future Microbiology*, *8*(9), 1129–1146. https://doi.org/10.2217/fmb.13.80
43. Ford, M. J., Harwalkar, K., Pacis, A. S., Maunsell, H., Wang, Y. C., Badescu, D., Teng, K., Yamanaka, N., Bouchard, M., Ragoussis, J., & Yamanaka, Y. (2021). Oviduct epithelial cells constitute two developmentally distinct lineages that are spatially separated along the distal-proximal axis. *Cell Reports*, *36*(10), 109677. https://doi.org/10.1016/j.celrep.2021.109677

44. Wira, C. R., Grant-Tschudy, K. S., & Crane-Godreau, M. A. (2005). Epithelial Cells in the Female Reproductive Tract: A Central Role as Sentinels of Immune Protection. *American Journal of Reproductive Immunology*, *53*(2), 65–76. https://doi.org/10.1111/j.1600-0897.2004.00248.x
45. Tian, Q., Zhang, T., Shu, C., Han, Z., Huang, Y., Wan, J., Wang, L., & Sun, X. (2024). Diverse animal models for Chlamydia infections: Unraveling pathogenesis through the genital and gastrointestinal tracts. *Frontiers in Microbiology*, *15*. https://doi.org/10.3389/fmicb.2024.1386343
46. Perlman, R. L. (2016). Mouse models of human disease. *Evolution, Medicine, and Public Health*, *2016*(1), 170–176. https://doi.org/10.1093/emph/eow014

APPENDIX A: METHODOLOGY

A.1 Intravaginal inoculation protocol

The intravaginal inoculation protocol that was utilized for this investigation was largely based off of a method previously described by Zhang et al (13). However, slight modifications were made to this method to ensure a reliable infection: 1) The inoculum was diluted to 10^5 IFUs/mL in 5µL of SPG instead of 2×10^5 IFUs/mL in 10µL of SPG, 2) After administering the inoculum, mice were held for 15 seconds instead of 2 minutes to avoid physical discomfort that would cause the mice to move and expel the inoculum, and 3) After extensive literature review and discussion with our collaborators, the Fields lab, we incorporated a pre-infection swab in order to clear the vaginal vault of mucus (30).

1. Prepare the *C. muridarum* inoculum by diluting purified EBs of the respective bacterial strain to a concentration of 10^5 IFUs in SPG buffer. SPG should be sterile filtered and pH tested. Vortex the diluted solution to ensure homogeneity of the sample, and place on ice until the time of inoculation.
2. Within the fume hood, using a p10 micropipette, load 5 µl of the diluted bacterial suspension and place the pipette adjacent to the workspace yet still within reach.

3. Upon performing a manual restraint, insert a sterile calcium alginate mini tipped swab into the vaginal vault of the female C57Bl/6 mouse. Rotate the swab 8 times counterclockwise and 8 times clockwise before removing the swab.
4. Using a clean paper towel, wipe away any urine from the genital area. Rearrange the mouse slightly so that its head is tilted downwards towards the work surface of the fume hood and its belly is facing upwards.
5. Insert the tip of the p10 micropipette loaded with *C. muridarum* into the vaginal vault of the mouse until the end of the tip comes into contact with the cervix. Slowly eject the inoculum into the vagina, reaching only the first stop on the pipette.
6. With caution, slowly remove the pipette from the vagina and place it aside. Continue holding the mouse in the declined position for 15 seconds to ensure that the inoculum does not exit the vaginal vault.
7. Place the mouse back into the cage and perform a brief health check by observing its behavior and movement in order to ensure its well being after the procedure.

A.2 Transcervical inoculation protocol

The transcervical inoculation protocol followed was previously developed by the Starnbach lab at Harvard University who specialize in transcervical *C. trachomatis* infections (5, 29).

1. Prepare the *C. muridarum* inoculum by diluting purified EBs of the respective bacterial strain to a concentration of 10^6 IFUs in SPG buffer. SPG should be sterile filtered and pH tested. Vortex the diluted solution to ensure homogeneity of the sample, and place on ice until the time of inoculation.
2. Place the NSET device onto a p10 micropipette and load 10 µL of the diluted *C. muridarum* suspension. Place the loaded pipette adjacent to the workspace yet still within reach.
3. Upon performing a manual restraint, insert a sterile speculum into the vagina of the mouse.
4. Using the loaded pipette, insert the tip of the NSET device through the speculum and thread the device into one of the uterine horns of the mouse. Carefully pipette the inoculum into the upper genital tract of the mouse before slowly removing both the NSET and the speculum.
5. Place the mouse back into the cage and perform a brief health check by observing its behavior and movement in order to ensure its well being after the procedure.

A.3 Vaginal swab protocol

Prior to beginning this investigation, vaginal swabs were not performed in the Lijek lab, largely because they are a technique performed after intravaginal

infection, and we most typically used *C. trachomatis* which is administered transcervically. Thus, to develop an effective means of vaginal shedding, I performed an extensive literature review, spoke with other labs, and troubleshooted a novel vaginal swab protocol. I leaned most heavily on existing methodology from Rixon et al., yet spoke with members from the Frietze lab at the University of New Mexico, and with Kenneth Fields at the University of Kentucky (31). To troubleshoot the swabs, we tried different swab materials, different glass beads, different buffers, and different collection techniques. The protocol we developed now serves as an effective means of measuring vaginal shedding throughout the course of infection, to be quantified by IFU analysis.

1. Pipette 500 μL of pH tested sterile filtered SPG buffer into labelled eppendorf tubes. Place tubes on ice until the procedure is ready to be performed. Using a serological pipette prepare a 50 mL conical containing 10 mL of SPG buffer.
2. Within the fume hood, place sterile calcium alginate micro-tipped swabs into the 50 mL conical containing SPG buffer, and soak the swabs for 15 minutes.
3. Upon performing a manual restraint, insert a soaked swab into the vagina of the mouse so that the tip of the swab is fully inserted within the vaginal vault. Rotate the swab 8 times counterclockwise and 8 times clockwise, sloughing off as many cells as possible in the process.

4. Slowly remove the swab and place it into the appropriately labelled eppendorf tube, cutting the long metal end of the swab with scissors so that it fits within the closed eppendorf tube. Place the tube with the swab immediately on ice.
5. Place the mouse back into the cage and perform a brief health check by observing its behavior and movement in order to ensure its well being after the procedure.
6. Add 2-3 sterile glass beads to the eppendorf tube, and vortex swabs for 5 minutes, ensuring that the swab comes into contact with the glass beads and does not remain stuck at the bottom of the tube.
7. From the vortexed solution, pipette 200 microliters into a new eppendorf tube to be sent out for IFU analysis by the Fields lab at the University of Kentucky. The remaining 300 microliters will be stored at -20˚ C until DNA extractions or further IFU analysis are performed.

A.4 DNA Extraction protocol

The DNA extraction protocol was performed by using the Qiagen DNeasy Blood and Tissue kit, using reagents and buffers from the kit and largely following along with their pre-prepared method. However, it was necessary to make modifications to the method in order to enhance DNA extractions and get the highest concentration yield. At the beginning of this study, the DNA extractions were largely unsuccessful, as DNA extracted from tissue samples had

extremely low concentrations. To account for this obstacle, we troubleshooted the DNA extraction protocol, modifying steps in order to refine our methodology and identify areas that may have been interfering with our results. We identified that the membranes of the spin columns from the Qiagen kit were malfunctioning, and thus turned to a new kit to address the problem. However, through the troubleshooting process we were able to identify areas in our existing DNA protocol that we could change in order to increase DNA concentration and purity. These changes included: 1) Placing our samples in the heat block overnight, 2) Incubating samples with ethanol at 4˚ C instead of at room temperature, 3) Allowing our samples to elute for 15 minutes instead of 5 minutes, 4) Initiating DNA extractions immediately after tissue collection to avoid a freeze/thaw cycle.

1. Pipette 100 µL of homogenate into labelled eppendorf tubes using a P1000 pipette.
2. Warm up the Buffer ATL slightly within the palms of the hands in order to prevent crystallization of the buffer. To the eppendorf, add 20 µL of Proteinase K and 80 µL of Buffer ATL. This step should be completed within the fume hood as aliquots contain *Chlamydia* infected tissues.
3. Vortex the eppendorfs briefly in order to mix, and place tubes within the thermocycler at a temperature of 56˚ C. Leave aliquots in the thermocycler to incubate overnight.

To be completed the next day

4. Take all tubes out of the thermocycler and add 200 µL of Buffer AL to each. Vortex tubes briefly to mix and incubate in the thermocycler at 56˚ C for 10 minutes.
5. After 10 minutes, remove tubes from the thermocycler and add 200 µL of 200 proof ethanol to each. Mix to vortex and incubate the tubes at 4˚ C for 5 minutes to allow for precipitation.
6. Remove tubes and pipette all samples into DNeasy mini spin columns placed within a 2mL collection tube. Centrifuge the spin columns at 6000 x g (8000 rpm) for 1 minute. Discard the flow-through and collection tube. Place the spin column into a new collection tube.
7. Add 500 µL of Buffer AW1 to the column and centrifuge at 6000 x g (8000 rpm) for 1 minute. Discard the flow-through and collection tube. Place the spin column into a new collection tube.
8. Add 500 µL of Buffer AW2 to the column and centrifuge at 20,000 x g (14,000 rpm) for 3 minutes. If the centrifuge cannot reach 20,000 x g set the centrifuge to the highest speed. Discard the flow through and collection tube.
9. Transfer the spin column to a new 1.5 mL eppendorf tube labelled with the experiment name, condition of the aliquot, and date. Elute the DNA by adding 100 µL of Buffer AE to the center of the spin column membrane. Incubate the tubes at room temperature for 15 minutes. Centrifuge the

tubes at 6000 x g (8000 rpm) for 1 minute. Remove the spin column and collect the eppendorf tube which contains the eluted DNA.

10. Nanodrop the eluate containing the extracted DNA and measure DNA concentration and purity to assess the integrity of the sample.
11. Store extracted DNA at -20˚ C for future analysis.

A.5 qPCR protocol

qPCRs were completed in accordance with a protocol previously developed by Rebeccah Lijek and a previous student in the Lijek Lab, Kyra Seiger.

1. Thaw all necessary reagents including buffers, primers, probe and DNA on ice. While reagents are thawing, calculate the necessary amount of each individual reagent required to prepare the 16S and GAPDH mastermix using the following base amounts:

16S qPCR Mastermix

	1X (uL)
2x buffer	12.5
F primer	0.3
R primer	0.3
probe	0.2

H2O	1.7

GAPDH qPCR Mastermix

	1X (uL)
2x buffer	12.5
F primer	0.6
R primer	0.6
probe	0.25
H2O	6.05

2. Set up 96-well plate plan, accounting for each DNA sample to be run in triplicate for both 16S and GAPDH.
3. Once reagents have thawed, prepare 16S mastermix using Taqman 2x buffer, 16S specific forward and reverse primers and probe, and deionized water. Place mastermix on ice.
4. Prepare GAPDH mastermix using Taqman 2x buffer, GAPDH specific forward and reverse primers and probe, and deionized water. Place mastermix on ice.
5. Add DNA to each individual well based off of the pre-designated plate plan. Place 10 uL of DNA in wells to which 16S mastermix will be added, and 5 uL of DNA in wells to which GAPDH mastermix will be added.

6. Add either 15 uL of 16S Mastermix or 20 uL of GAPDH Mastermix to each of their respective wells.
7. Seal Plate well and vortex to mix before spinning the plate down to collect the samples at the bottom of each well.
8. Load spun down plate onto AriaMX Real-Time PCR machine (Agilent Technologies), and confirm that the location of A1 on the plate is in alignment with the position of A1 on the machine.
9. Open AriaMX software on the qPCR machine, select FAM and VIC. Confirm plate set up, and confirm thermal cycling conditions to be:

    1. 50 deg C for 120 seconds
    2. 95 deg C for 600 seconds
    3. 2 step amplification (40 cycles)
    a. 95 deg C for 15 seconds
    b. 60 deg C for 60 seconds (acquire here!)
    4. melt curve

10. Upon confirmation, initiate the run. Once the run has completed, collect tabular results and graphical data.

APPENDIX B: Pathology Scoring Guidelines

Scorers: Aria Mallare, Akosua Frimpong, Ashna Mehta, Grace Wieselquist.

Scorers were trained by Rebeccah Lijek.

Scoring Procedure: Double anonymized scoring of H&E-stained tissue sections. Histopathology scoring criteria described below for each experiment. Slides were taped by a third party to ensure anonymity. Slides were then randomly divided amongst scorers, and assessed independently. Two scorers scored each slide, and after each slide was assessed, all scorers met for a consensus meeting. For cases in which both scores did not match, slides were re-evaluated under the microscope, and a third scorer broke the tie. Scores in which the tissue is missing, mostly missing, or altered in some way that made it difficult to score (e.g. missing bursa) are represented by an M or 'no score,' respectively.

Uterine Horn general pathology consistent with Lijek et al 2018 (5)

0 - No pathology

1 - Mild/rare pathology; less than 1/3 of tissue affected

2 - Moderate/multifocal pathology; between 1/3 and 2/3 of tissue affected

3 - Severe/coalescing pathology; greater than 2/3 of tissue affected

UT dilation consistent with Chen et al 2014 (35)

0 - No significant dilatation

1 - Mild dilation of a single cross section

2 - One to three dilated cross sections

3 - More than three dilated cross sections

4 - Confluent-pronounced dilation

Oviduct hydrosalpinx consistent with Chen et al 2014 (35)

0 - No hydrosalpinx

1 - Hydrosalpinx detectable visually but requiring microscopic confirmation

2 - Hydrosalpinx clearly visible with naked eyes but the size is smaller than the ovary on the same side

3 - Equal to the ovary on the same side

4 - Hydrosalpinx larger than the ovary on the same side

Cellular infiltration consistent with Chen et al 2014 (35)

0 - No significant infiltration

1 - Infiltration at a single focus

2 - Infiltration at two to four foci

3 - Infiltration at more than four foci

4 - Confluent infiltration

Preliminary Stage Scoring:

- Double anonymized scoring of H&E-stained tissue sections

- UTs: scored on 0-3 scale for severity of cellular infiltration

Uterine Pathology

0 - No neutrophil infiltration in lumenal spaces

1 - Less than 1/3 of tissue with neutrophil infiltration

2 - Between 1/3 and 2/3 of tissue with neutrophil infiltration

3 - Greater than 2/3 of tissue of tissue with neutrophil infiltration

*in some cases edema was taken into account if obvious (not common in this experiment)

- Oviducts: scored on a 0-2 scale for edema and cellular infiltration.
- Ovaries: scored on a 0-2 scale for edema and cellular infiltration.

Oviduct and Ovarian Edema

0 - No edema

1 - Mild/moderate edema

2 - Severe edema

Oviduct and Ovarian Cellular Infiltration

0 - No neutrophil infiltration in lumenal spaces

1 - Less than 1/2 of tissue with cellular infiltration

2 - More than 1/2 of tissue with cellular infiltration

*why this scale? We largely observed tissues with no edema/cellular infiltration or *severe* edema/cellular infiltration. There was really only one "in-between" phenotype (if not 0 or 2, there was *some* edema or some infiltrate).

- Analysis: unpaired t-test

Secondary Stage Scoring:

Acute Infection:

- Double blinded scoring of H&E-stained tissue sections
- UTs: scored on a 0-3 scale as in LHB1
- Oviducts: scored on a 0-2 scale for hydrosalpinx and cellular infiltration, same as LHB1
- Ovaries: scored on a 0-2 scale for edema and cellular infiltration, same as LHB1
- Analysis: no matching, nonparametric ANOVA

Chronic Infection

- Double blinded scoring of H&E-stained tissue sections
- UTs: scored on a 0-3 scale for general pathology consistent with Lijek et al 2018 and a 0-4 scale for dilation consistent with Chen et al 2014
- Oviducts: scored on a 0-4 scale for hydrosalpinx consistent with Chen et al 2014 and on a 0-2 scale for cellular infiltration as in LHB1

- Ovaries: scored on a 0-2 scale for edema and cellular infiltration as in LHB1
- Analysis: no matching, nonparametric ANOVA

APPENDIX C: Supplemental Figures

C.1 Additional Gross Pathology Images

A

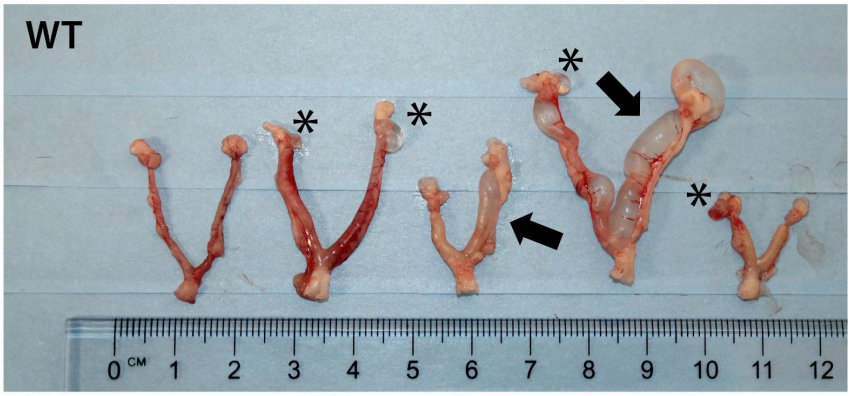

B

C

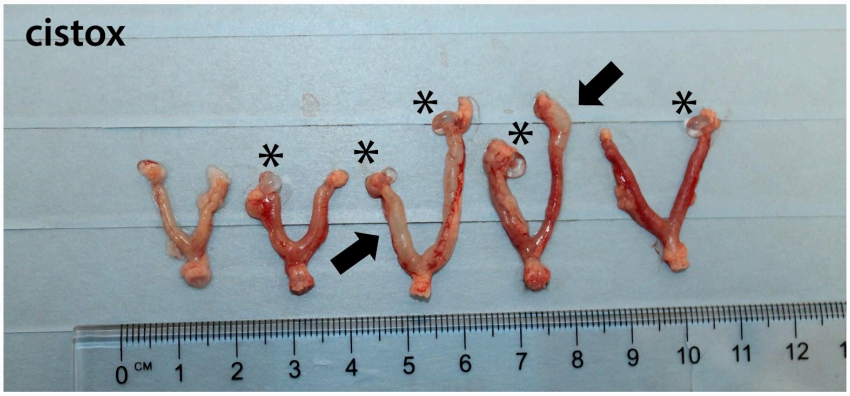

Supplemental Figure 1. Infection with Δtox results in reduced hydrosalpinx and uterine horn dilation. Gross pathology images of mouse genital tracts transcervically infected with the (A) WT, (B) Δtox, or (C) cistox strains of *C. muridarum* day 51 post transcervical infection. Presence of hydrosalpinx is indicated with a black asterisk, while presence of uterine distension is indicated with a black arrow. Images were taken on via an iPhone 11 camera.

C.2 Results of Intravaginal Pathology Assessment

For our comprehensive assessment of immunopathology in the secondary stage of this investigation, we chose to focus on how histopathology was altered during transcervical infection with the three different strains of the bacteria. The transcervical route was chosen, as our preliminary studies strongly suggested that upon intravaginal infection 1) Ascension to the upper genital tract was highly variable, and 2) a robust disease state that mimicked *Chlamydia* disease in humans did not occur. However, we did perform a similar experiment in which mice were challenged intravaginally and assessed for immunopathology on day 7 (acute) and day 51 (chronic) post infection. We found that there was no clear qualitative differences in both the gross pathology nor the histopathology of mice infected with the Δtox strains relative to the control. However, because of the unreliability of intravaginal challenge to elicit a robust upper genital tract infection, the results we observe do not accurately represent the infection phenotypes of the three strains.

A

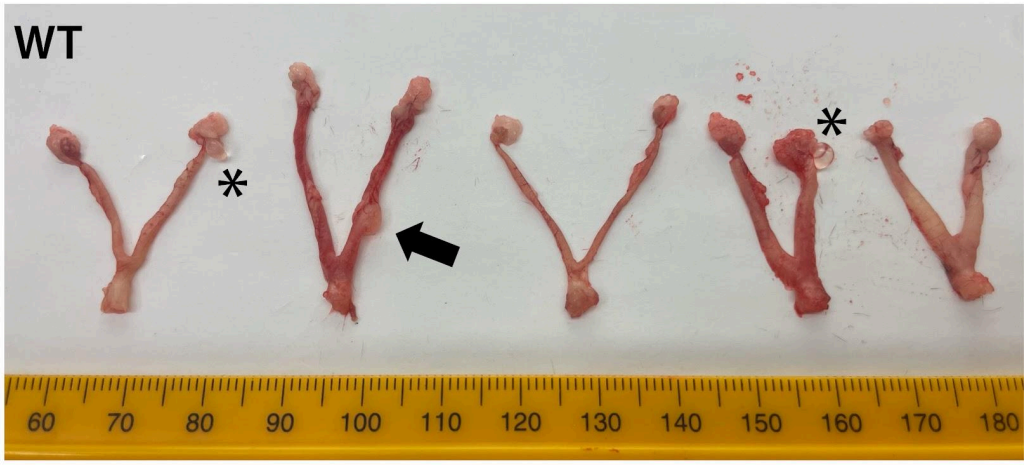
WT
60 70 80 90 100 110 120 130 140 150 160 170 180

B


Δtox
60 70 80 90 100 110 120 130 140 150 160 170 180 190

C

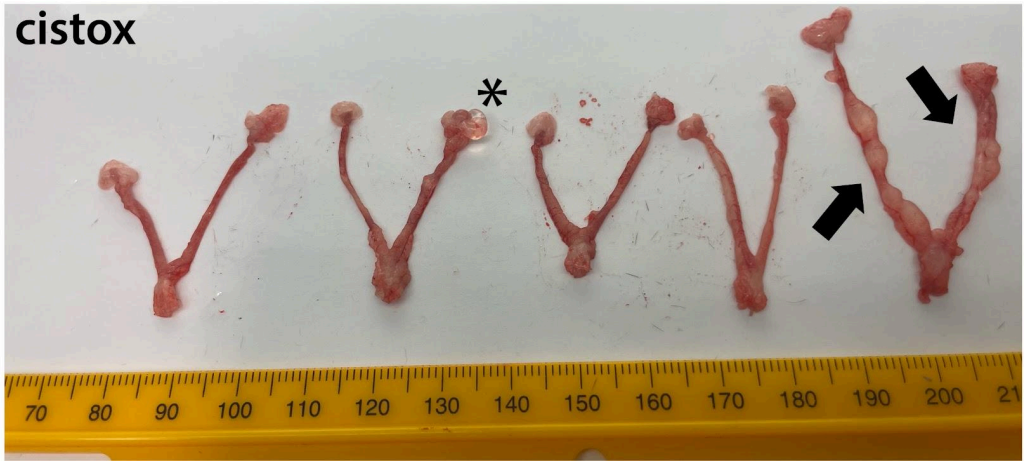
cistox
70 80 90 100 110 120 130 140 150 160 170 180 190 200

Supplemental Figure 2. Intravaginal infection with Δtox results in reduced hydrosalpinx development. Gross pathology images of mouse genital tracts intravaginally infected with the (A) WT, (B) Δtox, or (C) cistox strains of *C. muridarum* day 51 post transcervical infection. Presence of hydrosalpinx is indicated with a black asterisk, while presence of uterine distension is indicated with a black arrow. Images were taken on via an iPhone 11 camera.

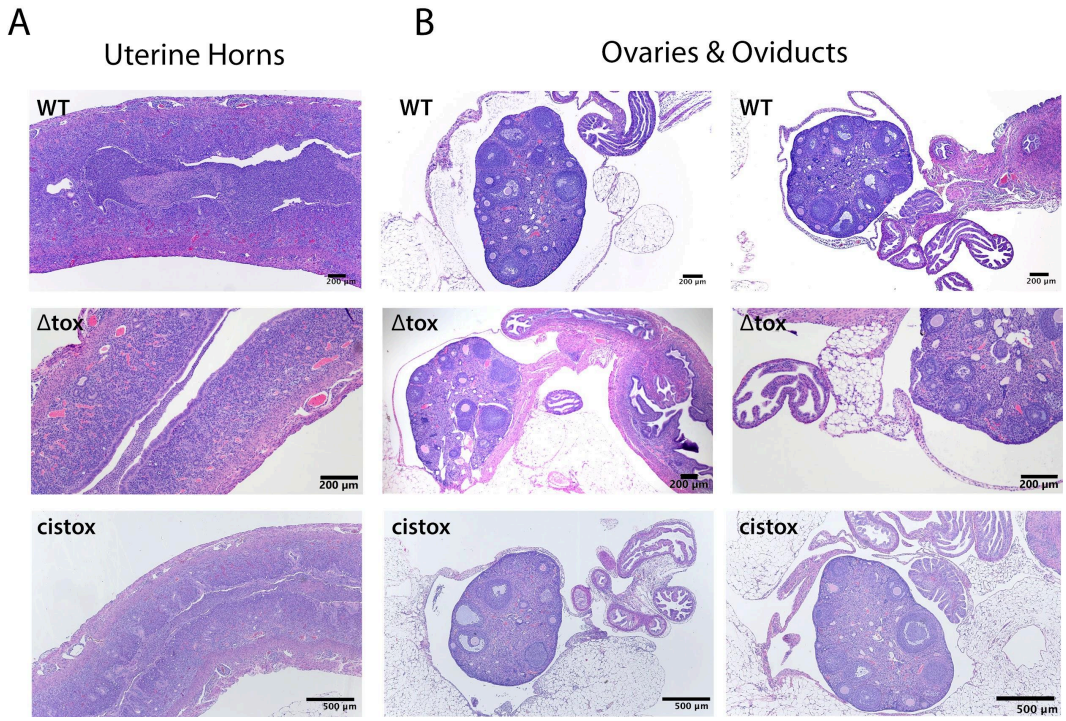

Supplemental Figure 3. Intravaginal infection with Δtox does not impact histopathology at acute timepoints. H&E stained mouse uteri (A), ovaries and oviducts (B) post transcervical infection with the WT, Δtox, or cistox strains of *C. muridarum*. Different rows indicate tissue infected with different strains. Genital tracts were excised on Day 7 post intravaginal infection, and sectioned and stained by the Harvard Rodent Histopathology core. Images were photographed via a Pixelink camera on a Nikon Eclipse 50i scope. Images were stitched together via cellSens imaging software and scale bars were added via ImageJ.

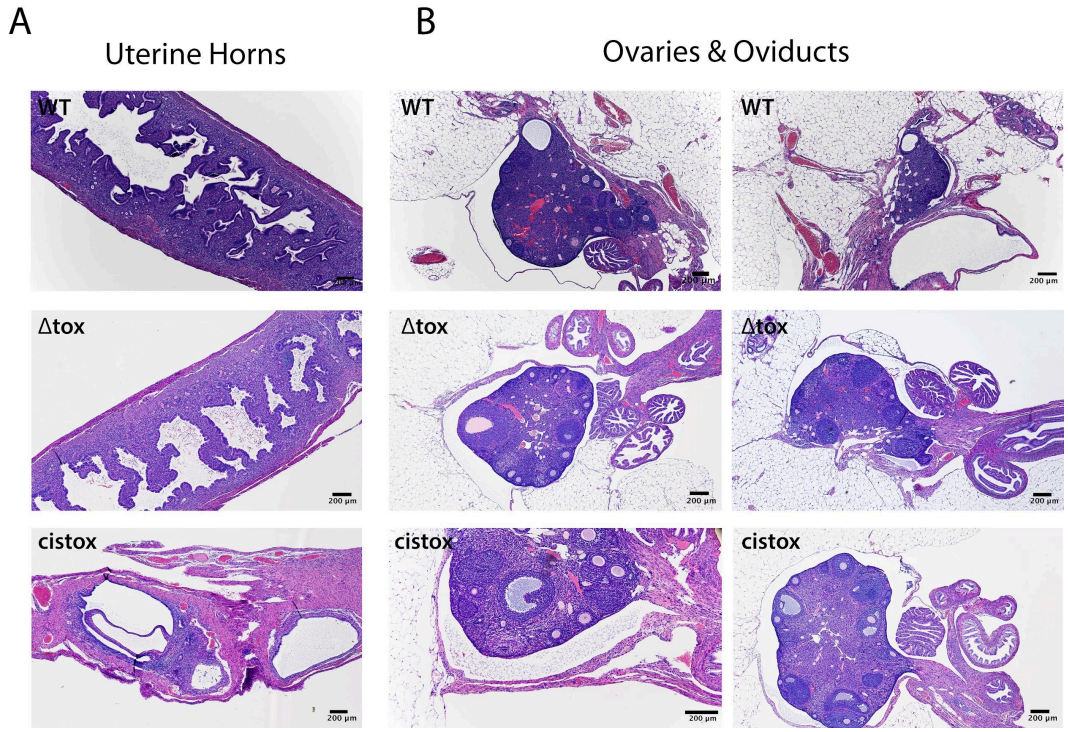

Supplemental Figure 4. Δtox does not impact histopathology after intravaginal infection at chronic timepoints. H&E stained mouse uteri (A), ovaries and oviducts (B) post transcervical infection with the WT, Δtox, or cistox strains of *C. muridarum*. Different rows indicate tissue infected with different strains. Genital tracts were excised on Day 51 post intravaginal infection, and sectioned and stained by the Harvard Rodent Histopathology core. Images were photographed via a Pixelink camera on a Nikon Eclipse 50i scope. Images were stitched together via cellSens imaging software and scale bars were added via ImageJ.

From our macroscopic, gross assessment of the tissue, we see that there is a reduction in the presence of hydrosalpinx and uterine distension in mice infected with the Δtox strain relative to the two control strains. At the cellular level, there is no difference in uterine horn or ovarian histopathology across the three strains, but there appears to be a slight reduction in oviduct pathology during chronic infection. WT infected mice exhibited mild oviduct edema and hydrosalpinx,

while Δtox infected mice did not. These findings align with what we saw upon transcervical infection, however, because of how variable ascension is upon intravaginal infection, we cannot reliably say that the phenotypes we observed are the result of the genomic composition of our three strains.

C.3 Δtox does not impact the ability of *Chlamydia* to persist in the upper genital tract.

As we saw during our assessment of vaginal shedding, the Δtox strain is cleared from the lower genital tract earlier than the control strains, suggesting that the ORFs play a role in bacterial persistence in the lower genital tract. To determine whether or not this was the case in the upper genital tract as well, we infected mice transcervically with the three strains of *C. muridarum* – Δtox, WT, cistox – and excised their upper genital tracts on day 51 post infection for qPCR assessment of bacterial burden.

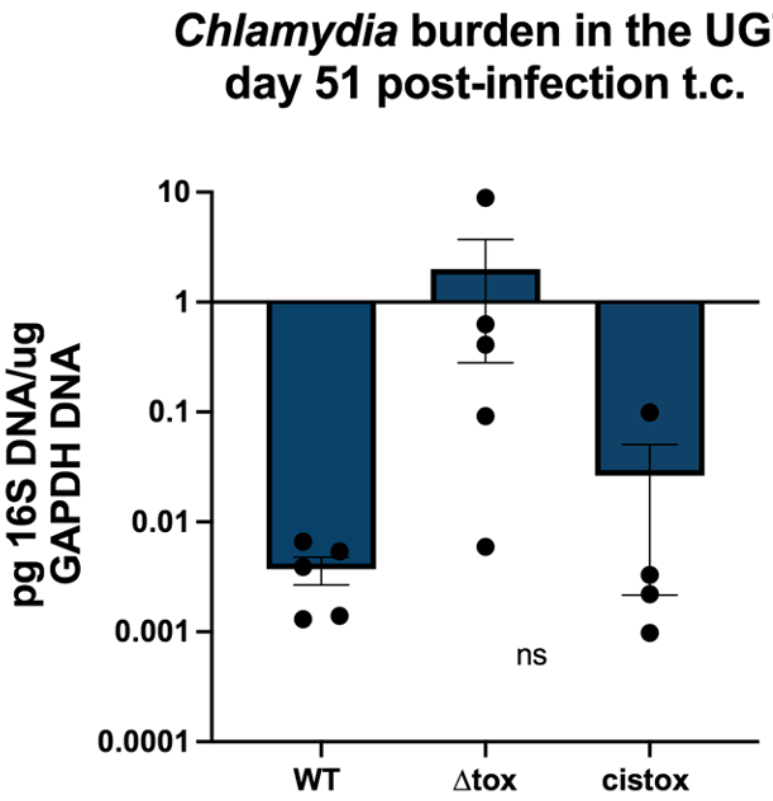

Supplemental Figure 5. Infection with Δtox does not impact *Chlamydia* upper genital tract burden at late time points. Upper genital tracts were harvested on day 51 post transcervical challenge, and bacterial burden was quantified via qPCR analysis of DNA extracted from UGT homogenates.

Supplemental Figure 4 indicates that upon upper genital tract infection, the Δtox strain is cleared at the same rate as the two control strains. Mice infected with all three strains had extremely low burdens, indicating that the absence of the ORFs from the *C. muridarum* genome does not impact the ability of the bacteria to persist in the upper genital tract to this late time point. The data displayed in this figure was only recently collected, and thus the necessary controls to precisely define our limit of detection of *Chlamydia* 16S DNA have not been run

yet. Without this limit of detection, we are unaware as to how much of the measured DNA is *Chlamydia* 16S DNA, and how much is background noise from the PCR technology or the host tissue of the sample. For data like this in which the burden value is so low, these controls are of the utmost importance, and thus these results do not necessarily accurately represent the results of our experiment. To define this limit of detection, the following controls will be run: 1) qPCR with no DNA template (Elution buffer to replace DNA), and 2) qPCR of an uninfected mouse homogenate. Upon running the controls, we will also run the necessary statistics, performing a one-way ANOVA followed by a Tukey's multiple comparisons test. In addition, it is important that we also look at other time points during transcervical infection to monitor bacterial persistence, as the vaginal shedding data indicated a difference in persistence at days 21 and 28 infection.